FUS/TLS was important for the interaction with SMN complexes and TDP-43 (Fig 2E and F). Furthermore, while FUS/TLS and TDP-43 proteins interacted with overexpressed HA-tagged SMN, they did not interact with SMN proteins that contained mutations in the tudor domain (W92S, G95R and E134K). These mutations are known to reduce affinity to RG repeats of Sm proteins and cause SMA (Tripsianes et al, 2011; Fig 2G). These results indicate that SMN associates with FUS/TLS and TDP-43 through an interaction between the tudor domain of SMN and the RGG domain of FUS. Therefore, three proteins implicated in motor neuron disease, TDP-43, FUS/TLS and SMN, interact with each other.

Loss of gems in motor neurons from ALS patients

Considering that Gems in human motor neurons differentiated from SMA patient-derived iPS cells are decreased compared with control (Ebert et al, 2009), it is very important to ask whether Gems are present in motor neurons of human spinal cords, and whether Gems are TDP-43-immunopositive. Post-mortem lumbar spinal cord tissues from ALS and non-ALS patients were stained. The accumulations that we observed of SMN and Gemin8, the two principal components of Gems in nuclei, indicated the presence of Gems in motor neurons from non-ALS human spinal cords (Fig 3A, arrows). Moreover, we found that TDP-43 localized to Gems in human motor neurons (Fig 3B, arrows). We quantified the number of Gems by double-staining for SMN and Gemin8, resulting in an average of 2.5 Gems per spinal cord motor neuron in control patients (Fig 3D). The average number of TDP-43-immunopositive Gems was 1.9 per spinal cord motor neuron in control patients (Fig 3E). Intriguingly, in motor neurons from ALS patients, with abnormal TDP-43 accumulation, Gemin8 was distributed uniformly throughout the nucleus and cytoplasm (Fig 3C). The quantification of numbers of Gems and TDP-43-positive Gems (0.08 and 0.06, respectively) revealed a significant loss of Gems in motor neurons from ALS patients (Fig 3D and E). The loss of Gems is also a feature of motor neurons from SMA patients, implicating the importance of Gem formation for motor neurons.

Alteration of U snRNA levels with TDP-43 depletion

The association and localization of TDP-43, FUS/TLS and SMN in Gems imply a functional convergence of three proteins. SMN is well known to assist in assembly of U snRNPs, which is central to splicing, in the cytoplasm and to recruit U snRNPs into the nucleus (Pellizzoni et al, 2002). In SMA mice and SMN-depleted cells, the levels of U snRNAs and components of U snRNPs are unbalanced, resulting in aberrant splicing (Gabanella et al, 2007; Zhang et al, 2008). Therefore, we hypothesized that TDP-43 might have a function in U snRNP biogenesis and alterations in U snRNPs may be also responsible for ALS. To test this hypothesis, we first analysed if TDP-43 associated with U snRNPs. TDP-43 distribution was similar to U snRNPs, which were marked by the anti-dimethylated Sm proteins antibody (Y12), and both TDP-43 and U snRNPs were concentrated to same nuclear bodies in Hela cells and primary cultured mouse hippocampal neurons (Fig 4A, arrows), suggesting the interaction of TDP-43 and snRNPs. Since C-terminus of TDP-43 is required for TDP-43-containing foci in nuclei (Fig 2B, Supporting Information Fig S3C), we identified proteins interacting with C-terminus of TDP-43. Comparison of proteins immunoprecipitated with wild type FLAG-tagged TDP-43 or deletion mutant of C-terminal domain, followed by LC–MS/MS, revealed many proteins associated with a TDP-43 C-terminus including U snRNP components such as PRPF3 (Supporting Information Fig S4A and B). The association of TDP-43 with U snRNP components PRPF3 and U1-70K was confirmed by IP-Western blotting (Supporting Information Fig S4C). To investigate the association between U snRNPs and TDP-43, U snRNPs were immunoprecipitated with the anti-Sm proteins antibody (Y12) (Supporting Information Fig S4D). Subsequent immunoblotting confirmed that TDP-43 was co-immunoprecipitated with U snRNPs although at a relatively low level. These results suggest a possible involvement of TDP-43 in maintaining the integrity of U snRNPs.

Next, we measured levels of U-rich small nuclear RNAs (U snRNAs), the major components of U snRNPs, following TDP-43 knockdown (Gabanella et al, 2007; Zhang et al,

Figure 2. Determination of domains required for association of TDP-43, FUS/TLS and SMN complex.

A. A schematic diagram of C-terminal 3XFLAG-tagged expression constructs for TDP-43 used in this study.

B. The latter half of the C-terminal glycine-rich region of TDP-43 was important for the proper localization to Gems. Hela cells were transfected with TDP-43-3XFLAG or indicated mutants, and stained with anti-SMN and anti-FLAG antibodies. Co-localization of TDP-43 and SMN was assessed by confocal microscope, numbers of TDP-43-positive Gems and -negative Gems were counted. More than 100 Gems were counted for each construct, and the localization to Gem (%) was defined as TDP-43-postive Gems per total Gems (%). To eliminate variation in the number of Gems per nucleus, cloned Hela cells were used. The average and error bars from three independent experiments were plotted.

C,D. The SMN/Gemin8/FUS interactions with TDP-43 were dependent on the TDP-43 C-terminus. TDP-43-3xFLAG mutants were expressed in Hela cells, and the TDP-43 interacting proteins were immunoprecipitated using an anti-FLAG antibody and identified by Western blot analysis using the specific antibodies as indicated. Asterisks indicate degraded FLAG-tagged TDP-43 proteins.

E. A schematic diagram of N-terminal 3XFLAG-tagged expression constructs for FUS/TLS used in this study.

F. 3xFLAG-FUS/TLS mutants were expressed in Hela cells, and the FUS/TLS interacting proteins were immunoprecipitated using an anti-FLAG antibody and identified by Western blot analysis using the specific antibodies as indicated.

G. Mutations in Tudor domain of SMN1 decreased association of TDP-43 and FUS/TLS. HA-tagged human SMN1 and its mutants were expressed in Hela cells, and SMN interacting proteins were immunoprecipitated using an anti-HA antibody and identified by Western blot analysis using the specific antibodies as indicated.

Figure 3. TDP-43-positive Gems are decreased in motor neurons from ALS patients.

A. Immunostaining of Gems in human spinal cord motor neurons. Paraffin-fixed post-mortem spinal cords from patients with neurological diseases other than ALS were analysed under a confocal microscope for the presence of Gems with antibodies against SMN and Gemin8 (Gem8) (arrows). Note that autofluorescence derived from lipofuscin was observed in the cytoplasm (asterisks). Bars: 10 μm.

B. Coimmunostaining of TDP-43 and SMN indicating the presence of TDP-43-positive Gems in human spinal cord motor neurons (arrows). Bars: 10 μm.

C. Coimmunostaining of TDP-43 and Gemin8 in remaining motor neurons of ALS spinal cords. TDP-43 is localized in the nucleus. Bars: 10 μm.

D. Nuclear foci with a significant concentration with Gemin8 and SMN were defined as Gem, and numbers of Gems in motor neurons from three control patients ($N = 21$) or three ALS patients ($N = 25$) were counted. Means are 2.476 and 0.08, respectively ($p < 0.0001$).

E. Nuclear foci with a significant concentration with Gemin8 as determined in (**D**) were defined as Gem, and numbers of TDP-43-positive Gems in motor neurons of spinal cords with control disease ($N = 19$) or ALS ($N = 18$). Means are 1.895 and 0.056, respectively ($p < 0.0001$).

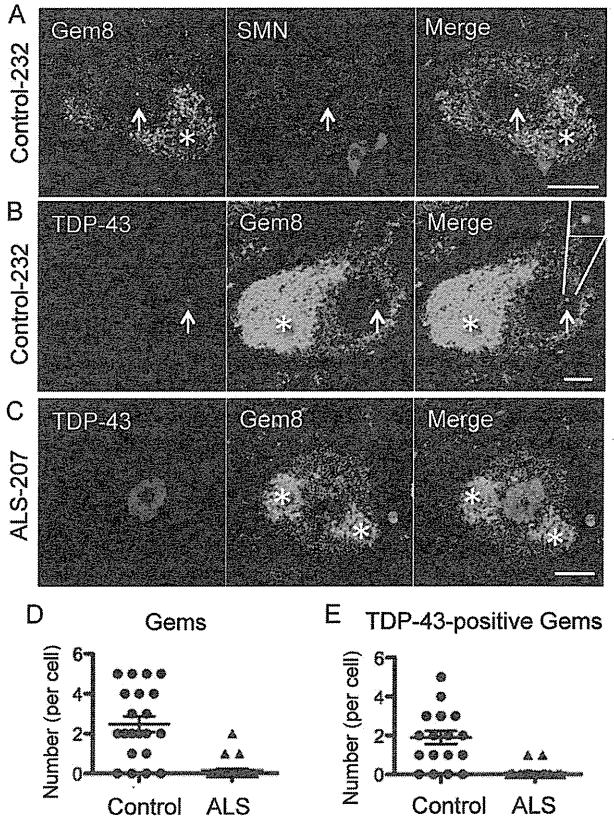

2008). Surprisingly, despite the lack of Gems, up-regulation of U snRNAs was observed in TDP-43 depleted cells. U2 snRNA levels were up-regulated in TDP-43 depleted Hela cells (Fig 4B), and U4, U5 and U6 snRNAs were up-regulated in TDP-43-depleted neuronal SH-SY5Y cells (Fig 4C). These results show that the dysfunction of TDP-43 causes misregulation of U snRNAs, although misregulated U snRNAs were different between these neuronal and non-neuronal cells. This is intriguing, because SMN-dysfunction causes cell-type specific misregulation of repertoires of U snRNAs, with decrease of distinct subsets of U snRNAs in different cell types (Gabanella et al, 2007; Zhang et al, 2008). We also measured levels of U snRNAs that are associated with mature U snRNPs in the nuclei of TDP-43 depleted cells, by immunopurification of U snRNPs from nuclei with the anti-Sm proteins antibody (Y12). The pattern of changes seen in U snRNA levels from mature U snRNP fraction (Fig 4D) was similar to that seen when U snRNAs were extracted from whole cells (Fig 4B). Therefore, the levels of U snRNAs associated with Sm proteins were up-regulated in the nuclei of TDP-43 depleted cells. Taken together, these data indicated that TDP-43 is important for maintaining the proper levels of U snRNAs.

U snRNA levels are aberrantly upregulated in ALS, but not in FTLD

Since an abnormal disappearance of TDP-43 from nuclei was observed in motor neurons from sporadic ALS patients and Gems were lost in these neurons (Fig 3) and TDP-43 was important for maintaining the proper integrity of spliceosome U snRNPs (Fig 4), we thought it would be of high interest to investigate whether U snRNA and U snRNP misregulation occurs in affected regions of ALS patients. Frozen cervical spinal cords from four sporadic ALS patients, with spinal cords from five other neurological disease patients serving as controls, were analysed for levels of U snRNAs and other mRNAs. Detailed clinical information is listed in Supporting Information Table S1. Almost all U snRNAs were upregulated in the spinal cords of ALS patients when compared with the control spinal cords (Fig 5A and B). This result confirms that the misregulation of U snRNA levels occurs in the affected region of ALS patients.

We next investigated whether this dysregulation occurs specifically in affected motor neurons in spinal cords of ALS patients. To this end, we stained spinal cords with an anti-2,2,7-trimethylguanosine (TMG) antibody that recognized the 5′ cap structure of U snRNAs. This staining revealed strong accumulations of U snRNAs in motor neurons from ALS patients. TMG staining was higher in motor neuron nuclei from ALS spinal cords than in nuclei from control spinal cords (Fig 5C and D). These results demonstrate that U snRNAs are upregulated in affected motor neurons from ALS patients.

We further asked whether these alternations in U snRNA levels would be seen in the affected regions of patients with other diseases with TDP-43 dysfunction, such as FTLD-TDP. Expression levels of U snRNAs in the temporal lobes of FTLD-TDP patients were analysed by both quantitative RT-PCR and immunohistochemistry using anti-TMG antibody. We found that they were not significantly altered compared with those in control patients (Supporting Information Fig S5A–C). Aberrant strong TMG staining was not observed in neuronal nuclei in FTLD-TDP temporal lobes, despite TDP-43 pathology. Moreover, analyses of long non-coding RNA (lnc RNA) levels

demonstrated that NEAT1, which is the most upregulated RNA substrate of TDP-43 in FTLD-TDP affected regions (Tollervey et al, 2011), was not upregulated in ALS spinal cords (Supporting Information Fig S6A–D). These results indicate that the patterns of snRNA/lncRNA dysregulation in neurons with TDP-43 depositions differ among distinct neuronal cell types, and the strong up-regulation of U snRNAs in nuclei is prominent in motor neurons from ALS spinal cords but not in FTLD-TDP temporal lobes.

Abnormal accumulation of U snRNPs in motor neuron nuclei of ALS spinal cords

We further investigated whether protein components of U snRNPs were also altered in motor neurons from ALS patients' spinal cords as well as snRNAs, the RNA components of snRNPs. The detailed analysis using immunofluorescent staining with anti-TDP-43 and anti-Sm proteins (Y12) antibodies reveals the accumulation of TDP-43 and snRNPs in the same nuclear body in nuclei of some motor neurons (Fig 6A, arrow) as seen in cultured cells; however, the staining intensity of the anti-Sm proteins (Y12) antibody in nuclei was very weak compared with that seen in cultured cells (Fig 4A). In ALS motor neurons, U snRNPs were extensively accumulated and formed aberrant aggregates in nuclei (Fig 6B–D, and Supporting Information Fig S7), as seen with anti-TMG antibody (Fig 5C and D). Immunohistochemistry also confirmed striking accumulation of U snRNPs in ALS motor neuron nuclei (Fig 6E), but not in nuclei of hippocampal neurons from FTLD-TDP patients (Supporting Information Fig S5D–F). The quantification analysis of the Y12 staining in motor neurons from four control patients and three ALS patients revealed that aberrant U snRNPs accumulation was highly specific to ALS motor neurons (Fig 6F). This abnormal nuclear accumulation of spliceosomal U snRNPs as well as snRNAs could lead to abnormal splicing in ALS motor neurons, resulting in neurodegeneration (Fig 6G).

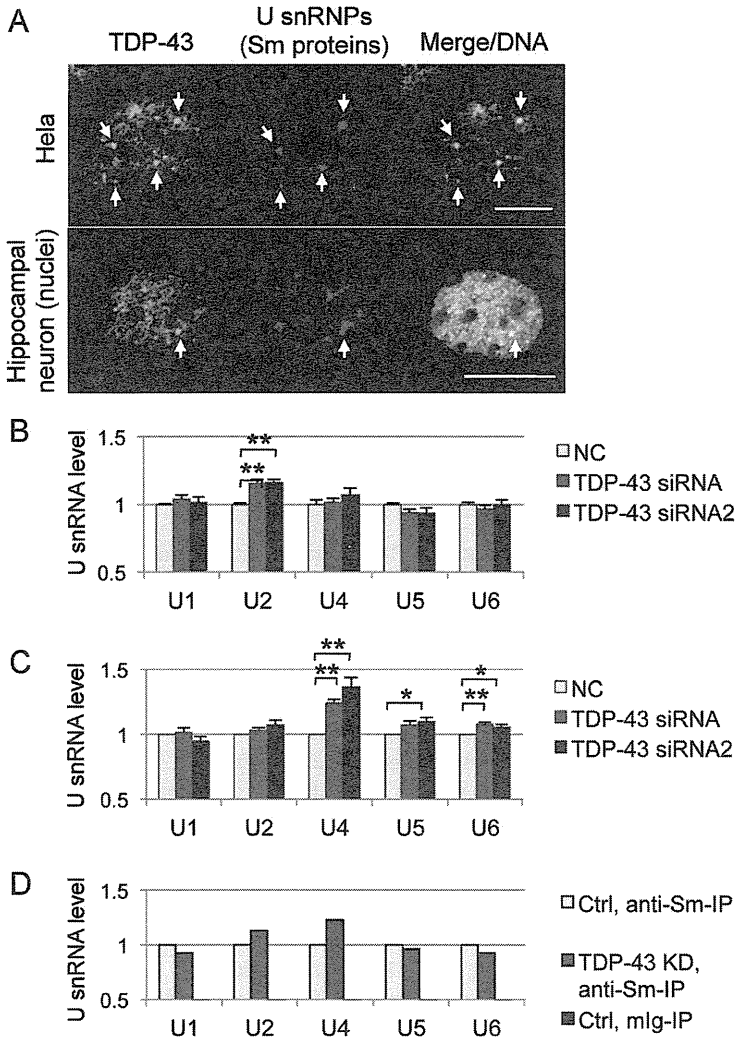

Figure 4. TDP-43 is associated with U snRNPs and is required for maintaining proper expression levels of U snRNAs.

A. TDP-43 colocalized with U snRNPs that were marked with an anti-dimethylated Sm proteins antibody (Y12) in the nuclei of Hela cells and primary cultured mouse hippocampal neurons. Note that U snRNPs and TDP-43 were concentrated in the same nuclear bodies (arrows). Bar: 10 μm.

B,C. U snRNA levels in Hela cells (**B**) or SH-SY5Y cells (**C**) treated with siRNAs for TDP-43 or control were determined by quantitative RT-PCR. Average from three independent experiments with transfections performed in triplicate were plotted (Bars: standard errors, $^{*}p < 0.05$, $^{**}p < 0.01$, Student's *t*-test).

D. Mature U snRNP-associated U snRNA levels in Hela cells treated with siRNAs for TDP-43 or control. U snRNA levels were determined by quantitative RT-PCR from the RNAs isolated from mature U snRNP complex which was immunopurified using anti-Sm proteins antibody (Y12) as described in Materials and Methods.

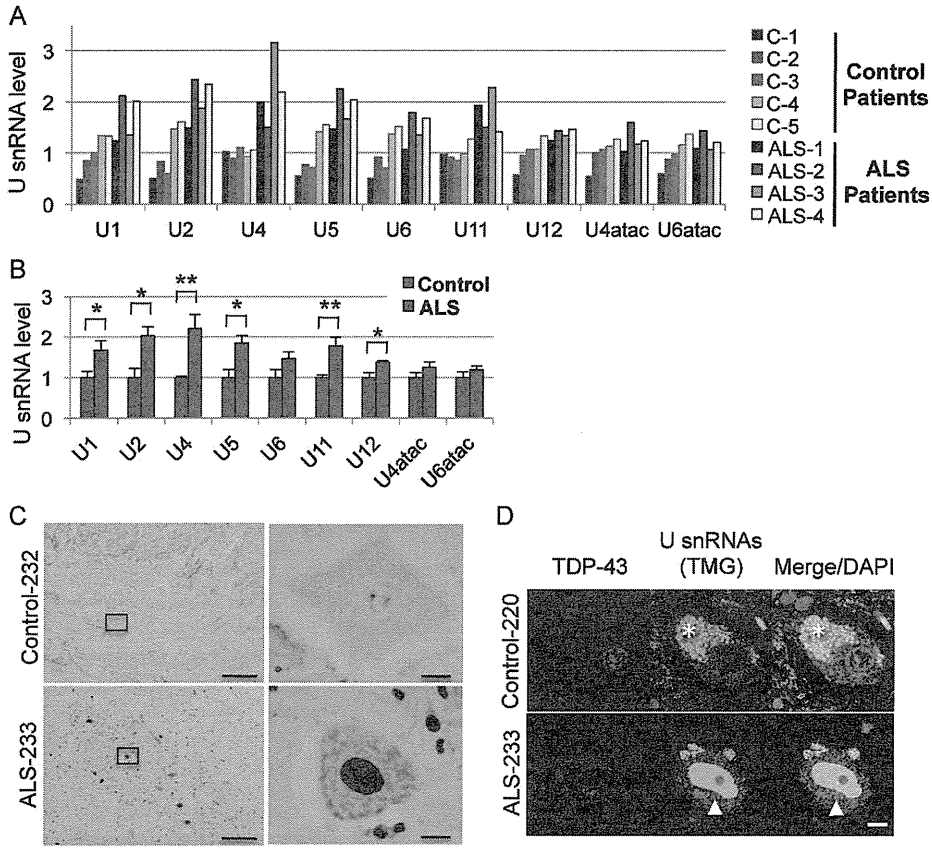

Figure 5. Expression levels of U snRNAs are up-regulated in cervical spinal cords of ALS patients.

A. The RNAs were isolated from cervical spinal cords of four ALS patients (ALS-1 to ALS-4) or five control patients with other neurological disease (C-1 to C-5), and U snRNA levels were determined by quantitative RT-PCR as in Fig 4. Detailed clinical information is listed in Supporting Information Table S1.

B. Mean U snRNA levels of control and ALS patients determined in **A** were plotted. Average amounts of U snRNAs from the five control patients were used for normalization. Robust U snRNA misregulation was observed in ALS patients. (Bars: standard errors, $^{*}p < 0.05$, $^{**}p < 0.01$, Student's *t*-test).

C. Immunohistochemistry of spinal cords from patients with control disease or ALS using an anti-2,2,7-trimethylguanosine (TMG) antibody, which recognized the 5′ cap structure of snRNA. Boxed areas were shown as the magnified images (Right panels). Bars: 500 μm (left), 20 μm (right).

D. Immunofluorescence staining of spinal motor neurons using anti-TMG and anti-TDP-43 antibodies. Note that strong accumulation of U snRNAs in nucleus of motor neurons from ALS patients (arrowheads). Asterisks show autofluorescence derived from lipofuscin in the cytoplasm. Bars: 10 μm.

DISCUSSION

In this study, we show that TDP-43 localizes to Gems through an association with an SMN/FUS complex and is critically involved in Gem formation and spliceosome maintenance by controlling U snRNA levels. Dysfunction of these proteins impairs the spliceosome resulting in abnormal splicing in motor neurons and neurodegeneration (Fig 6G). We also show that TDP-43 and SMN-dependent spliceosome dysregulation is common to the motor neuron diseases ALS and SMA, respectively, but not FTLD-TDP. In tissue from sporadic ALS patients, or following TDP-43 knockdown in cells, nuclear Gems collapsed and expression levels of U snRNAs spliceosome components were aberrantly up-regulated. Furthermore, U snRNPs aberrantly accumulated in motor neuron nuclei from ALS patients, but not in temporal cortex neurons from FTLD-TDP patients. Our findings strongly indicate that abnormal U snRNP level, which can cause abnormal RNA splicing and/or isoform expression (Berg et al, 2012), is an important mechanism resulting in neurodegeneration common to the motor neuron diseases ALS and SMA (Fig 6G).

The most provocative findings in our study revealed that U snRNA misregulation was observed in several distinct contexts: cells with a decreased expression of TDP-43 (Fig 4B–D) and spinal cord tissue samples of ALS patients (Fig 5), but not in the affected brain regions of FTLD-TDP (Supporting Information Fig S5A and B). Cell type- or tissue- specific alterations in U snRNA repertoires were identified in cells with low levels of SMN and in SMA mouse tissues (Gabanella et al, 2007; Zhang et al, 2008). Similarly, we observed that different sets of U snRNAs were misregulated in neuronal and non-neuronal cells following TDP-43 depletion. Although the direction of U snRNAs misregulation is different between the two diseases; upregulated U snRNAs in ALS, and downregulated U snRNAs

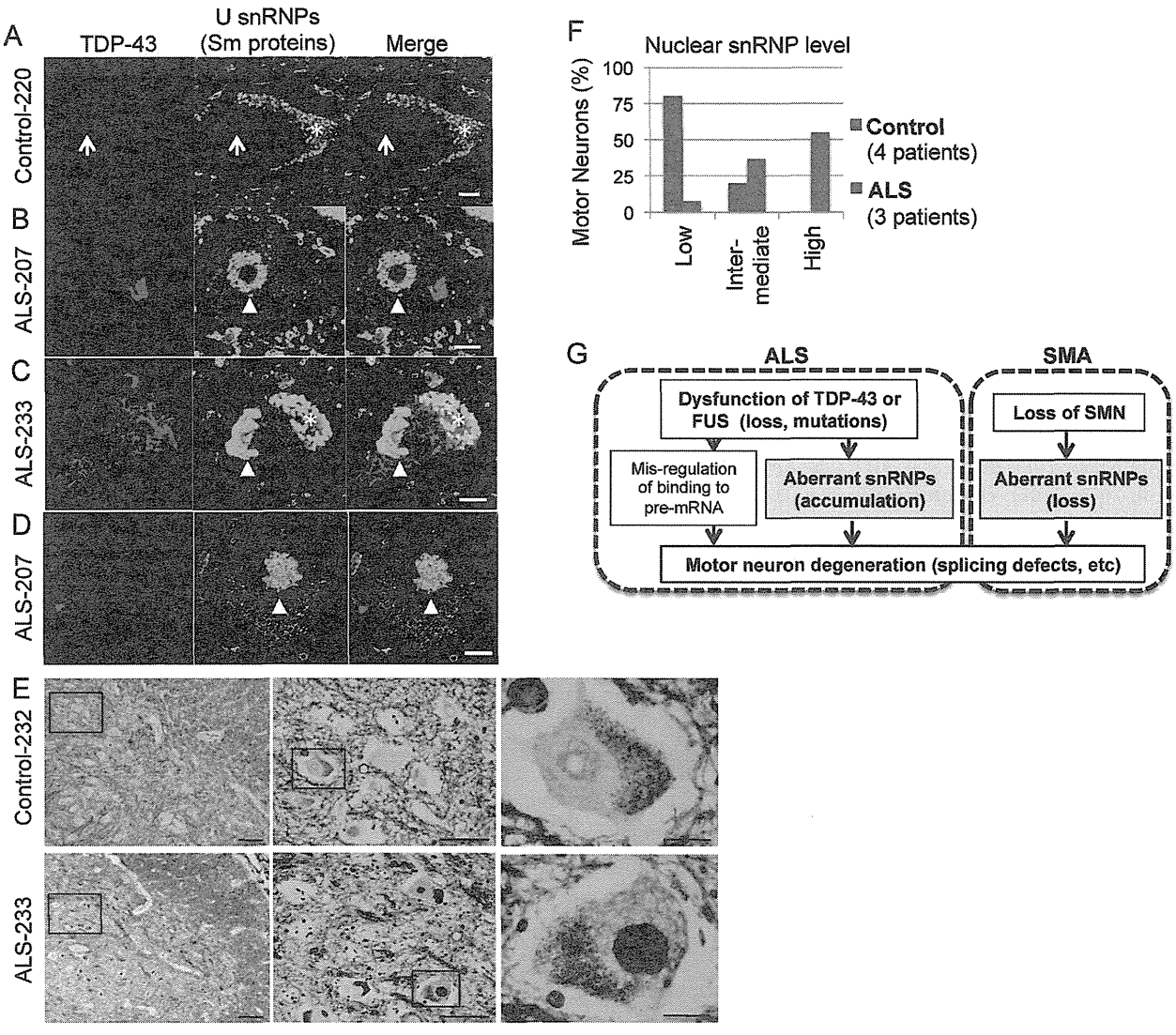

Figure 6. Abnormal accumulation of U snRNPs in motor neuron nuclei of ALS patients.

A–D. Immunofluorescent staining of TDP-43 and U snRNPs using an anti-Sm proteins antibody (Y12) in spinal cord motor neurons from patients with control diseases (**A**) or ALS (**B–D**). Arrow shows colocalization of the Y12 antigen and TDP-43 (**A**). The Y12 antigen accumulated in nuclei of ALS motor neurons with TDP-43 mislocalization (**B–D**). Arrowheads (**B–D**) show accumulated U snRNPs in motor neuron nuclei from ALS patients. Asterisks show autofluorescence derived from lipofuscin in the cytoplasm. Bars: 10 μm.

E. Immunohistochemistry of U snRNPs using an anti-Sm proteins antibody (Y12) in spinal cord motor neurons from patients with control diseases or ALS. Boxed areas in the left and middle panels were shown as the magnified images in the middle and right panels, respectively. Bars: 500 μm (left), 100 μm (middle), 20 μm (right).

F. Quantification of U snRNP immunofluorescence levels in motor neuron nuclei. Motor neurons from four control patients (blue, $N = 35$) and three ALS patients (red, $N = 105$) were analysed for U snRNP fluorescence intensity in their nuclei. The level of fluorescence intensity of U snRNPs in nuclei compared with cytoplasm were classified as low (nuclear U snRNP level is lower than cytosol), intermediate (nuclear U snRNP level is equal to cytosol), or high (nuclear U snRNP level is higher than cytosol), and plotted. Representative images of motor neurons showing low, intermediate or high nuclear U snRNP levels are shown in Supporting Information Fig S7.

G. Model for mechanism underlying neurodegeneration in ALS with dysfunction of TDP-43 in comparison to SMA. In this study, we show that TDP-43 localizes in nuclear Gem through association with SMN complex, and is involved in maintenance of spliceosome through controlling the levels of U snRNAs. In ALS patients and SMA mice, U snRNA levels are misregulated in spinal cord. Intriguingly, accumulation of U snRNA is seen in ALS, while loss of U snRNAs is reported in SMA. Moreover, Gems are lost and spliceosomal U snRNPs abnormally accumulate in nuclei of motor neurons from ALS patients. These findings indicate collapse of spliceosome integrity is the critical process common to motor neuron degeneration in ALS and SMA, and may explain cell-type specific vulnerability in motor neurons.

in SMA, our work is the first to imply that motor neurons may be sensitive to the collapse of spliceosome, resulting in abnormal splicing through alteration of U snRNP levels (Fig 6). Interestingly, transgenic mice overexpressing poly-Q binding protein-1, which binds to the U5 snRNP component, under a ubiquitous promoter show a late-onset motor neuron disease-like phenotype (Okuda et al, 2003; Waragai et al, 2000). Therefore, motor neurons might be sensitive to snRNP alterations, which would be a potential target for the therapy of motor neuron diseases.

Our results clearly indicate that TDP-43 and SMN might function in a common pathway, namely the regulation of splicing through the maintenance of U snRNP repertoires. Previous studies have demonstrated a genetic link between ALS and SMA. Aberrant copy numbers of SMN1 or SMN2 genes increase the risk of sporadic ALS and disease severity (Andersen & Al-Chalabi, 2011; Blauw et al, 2012; Corcia et al, 2006; Veldink et al, 2001, 2005). Our observation that TDP-43 regulates U snRNAs and associates SMN complex suggests a major function shared between TDP-43 and SMN and supporting a genetic link between ALS and SMA.

Recent studies identifying RNA targets of TDP-43 (Polymenidou et al, 2011; Sephton et al, 2011; Tollervey et al, 2011; Xiao et al, 2011) demonstrated that TDP-43 directly binds to some pre-mRNAs to regulate RNA splicing. However, not all TDP-43 binding sites in pre-mRNAs (as determined by CLIP-seq) are located close to splicing sites, suggesting that TDP-43 might regulate splicing through both direct binding to pre-mRNA and other mechanisms. Our study suggests that TDP-43 also regulates spliceosomal U snRNP biogenesis, which would provide another mechanism of TDP-43-mediated regulation of splicing. Abnormal splicing in motor neurons from ALS patients was reported before (Rabin et al, 2010), however, we are not able to correlate abnormally spliced genes in ALS with abnormal U snRNA repertories at present. The genes indispensable for motor neuron survival may be identified in the future by comparing the numerous abnormally spliced genes reported in SMA with the same genes in ALS.

Although U snRNAs were upregulated only about twofold in the whole spinal cord by quantitative RT-PCR, intense U snRNA staining in ALS motor nuclei indicates much higher U snRNAs upregulation in ALS motor neuron nuclei (presumably more than 100-fold, considering the number of motor neuron much smaller than that of the other spinal cord cell types; Fig 5C and D). Moreover, U snRNAs accumulate and sometimes form aggregates with proteins (Fig 6A–E). Therefore, we speculate that the abnormal accumulation of U snRNPs (they are likely to be non-functional) in ALS motor nuclei could have a substantial impact on RNA splicing and metabolism in motor neurons.

We discovered that TDP-43 and FUS/TLS localizes to nuclear Gems and that Gems are lost in motor neurons of spinal cords from ALS patients as well as TDP-43 depleted or FUS/TLS knockout cells. This is similar to observations in SMA patient-derived cells and SMA mouse models. The number of Gems is correlated with SMA disease severity in fibroblast from SMA patients (Coovert et al, 1997). Furthermore, a recent study showing a reduced number of Gems in the fibroblasts from familial ALS cases with TDP-43 or FUS mutations (Yamazaki et al, 2012) strengthens our findings on the importance of Gem in motor neuron survival. U snRNPs are thought to be stored in Gems for recycling; therefore, TDP-43 might be important for the maintenance of U snRNPs in Gems. The relationship between Gems and TDP-43 has been investigated in several studies. One study demonstrated that the alternatively spliced minor form of mouse TDP-43, which is lacking the C-terminal portion, interacted with SMN (Wang et al, 2002). Another study demonstrated the co-localization of full-length TDP-43 and SMN in human non-neuronal cells (Fiesel et al, 2010), however, additional studies claimed that the colocalization of TDP-43 and SMN was not detected in rat and mouse neurons (Casafont et al, 2009; Shan et al, 2010). In contrast, our study clearly demonstrated that endogenous human TDP-43 was localized in Gems of cultured cells and human motor neurons by coimmunostaining with TDP-43, SMN and Gemin8 (Fig 1A–E and 3). The loss of Gems seen in motor neurons of ALS patients (Fig 3), coupled with the fact that eliminating TDP-43 from mouse neurons *in vivo* leads to the loss of Gems (Shan et al, 2010), clearly supports our findings that TDP-43 and perhaps FUS/TLS is important for Gem formation and U snRNPs biogenesis, as observed before in a similar way with SMN. Furthermore, SMA mutations in the tudor domain of SMN, which is crucial for binding to Sm proteins, abolished SMN association with TDP-43 and FUS/TLS (Fig 2G), supporting an importance of SMN/TDP-43/FUS complex in the biogenesis of spliceosome and in motor neuron degeneration. Moreover, profilin1, which binds to SMN and localizes to Gem (Giesemann et al, 1999), was recently discovered as an ALS causative gene product (Wu et al, 2012). Overexpression of an ALS causing-mutant SOD1 prevents the formation of Gem in the motor neurons of mice (Kariya et al, 2012). Therefore, abnormal Gem formation and/or abnormal U snRNPs formation may underlie the mechanisms of motor neuron degeneration.

The importance of the C-terminal region of TDP-43 was demonstrated through the identification of a domain required for the proper targeting of TDP-43 to Gems and association with SMN (Fig 2A–D), and also by the identification of interactions with several proteins implicated in RNA metabolism (Supporting Information Fig S4). TDP-43 associated with various proteins implicated in RNA metabolism, including proteins involved in pre-mRNA splicing, translational control and the miRNA pathway. Considering that most ALS-linked mutations reside in the C-terminus of TDP-43 (Lagier-Tourenne & Cleveland, 2009), C-terminal region-mediated regulation of RNA metabolism may be disturbed in motor neuron diseases. The proteins we identified could therefore be important to analyse for further potential contributions to motor neuron degeneration.

It is intriguing that TDP-43 localized not only to Gems but also to paraspeckles and nuclear speckles. The long non-coding RNA (lncRNA) NEAT1 (also called Men ε/β) is indispensable for the formation of paraspeckles, where highly edited mRNAs are stored (Bond & Fox, 2009). Furthermore, nuclear speckles are enriched with spliceosomal U snRNPs, other splicing regulators important for RNA splicing such as SR proteins and Malat1

lncRNA (Mao et al, 2011). The expression of NEAT1 and Malat1 lncRNA, both of which have multiple TDP-43 binding sites, is elevated in FTLD-TDP brain (Tollervey et al, 2011). Our study with FTLD-TDP patients also demonstrated an increased expression level of NEAT1 (Supporting Information Fig S6B and D). However, NEAT1 was not significantly altered in ALS spinal cord and TDP-43 depleted cells (Supporting Information Fig S6A and C), suggesting distinct regulations of this lncRNA in different disease conditions. Nevertheless, the enrichment of TDP-43 in paraspeckles and speckles should be examined further to determine any potential role in RNA metabolism in these nuclear subdomains. Taken together, the expression of U snRNA spliceosome components was aberrant and long non-coding RNAs were normal in ALS spinal cords, but these profiles were reversed in FTLD. These results suggest that while neurodegenerative diseases with distinct causal genes (ALS, SMA) can have disruptions in a common biochemical pathway, diseases with the same causal gene (ALS, FTLD) can also have disruptions in distinct pathways.

In conclusion, we show here that TDP-43 and SMN share a common function in spliceosomal U snRNP biogenesis. Dysfunction of these distinct proteins in ALS and SMA leads to collapse of spliceosome integrity and abnormal splicing in motor neurons. We expect that further investigation of defects in RNA metabolism common to these motor neuron diseases but different from a related brain disease should provide explanation to the cell-type specific vulnerability observed in neurodegenerative diseases. In addition, targeting spliceosome and/or Gem stability in motor neurons may represent a new class of candidate therapeutics for motor neuron diseases.

MATERIALS AND METHODS

Expression vectors

The open reading frame of human *TARDBP* was inserted into p3XFLAG-CMV14 vector (Sigma), resulting in the insertion of an 18 amino acid spacer between the TDP-43 C-terminus and 3XFLAG peptides. Coding regions of TDP-43 fused with 3xFLAG were subcloned into pF5K-CMV-neo vector (Promega). For FUS/TLS expression, the open reading frame of human *FUS/TLS* fused with 3XFLAG on its N-terminus were subcloned into pF5K-CMV-neo or pF5A-CMV-neo vector (Promega).

Cell culture and immunofluorescence

Hela cells were maintained in DMEM with high glucose (Gibco) supplemented with L-glutamine, and 10% foetal bovine serum (Gibco). SH-SY5Y cells were maintained in Advanced DMEM/F12 (Gibco) with non-essential amino acids, sodium pyruvate, GlutaMAX (Gibco), and 10% foetal bovine serum. Hippocampal neurons were isolated from E16.5 C57BL6 or *FUS*$^{-/-}$ mouse embryos and cultured essentially as described (Huang et al, 2007). Cells were cultured on chamber slides (Lab-Tek, Nunc), fixed with 4% paraformaldehyde for 10 min and permeabilized with 0.1% Triton X-100. For paraspeckle staining with mouse anti-p54 (BD transduction), cells were fixed with cold methanol. Non-specific binding was blocked by incubation with 1% normal goat serum prior to the application of primary antibody. Antibodies used were as follows: rabbit anti-TDP-43 (ProteinTech), anti-coilin (Sigma, clone pδ), mouse anti-p54 (BD transduction), anti-SRSF2 (Sigma, clone SC-35), mouse anti-SMN (BD transduction, 610646), rabbit anti-SMN (Santa Cruz, sc-15320), mouse anti-Gemin8 (Santa Cruz, sc-130669), rabbit anti-FUS/TLS (Abcam, 70381), anti-dimethylated Sm proteins (Lab Vision Corp./Thermo Scientific, clone Y12), anti-TMG (Santa Cruz, clone K121), mouse anti-FLAG (M2), rabbit anti-FLAG (Sigma) and rabbit anti-GFP (MBL).

Knockdown of protein expression in cells

To eliminate TDP-43 expression, Hela cells were transfected with 4 nM Stealth siRNA for *TARDBP* (Invitrogen, ID#HSS177422 or originally designed oligos with the sequences listed in Supporting Information Table S2) or control siRNA (Invitrogen, LoGC#2 or #3) in suspension at 1.5×10^5 cells/ml using Lipofectamine RNAiMax (Invitrogen). After an overnight culture, cells were then transfected with siRNA once more, and then cultured for two more days. For SH-SY5Y cells, cells were transfected in suspension at 3×10^5 cells/ml. After 3 days of culture, cells were divided into three dishes, transfected with siRNAs again and cultured for three more days.

Immunoprecipitation

Cells were transfected with pF5K-TDP-43-3xFlag constructs using X-tremeGENE HP (Roche). Cells were harvested and washed with PBS 3 times. TBS supplemented with 0.2% Triton X-100, protease inhibitors (Nakalai, Japan), and RNase inhibitor SUPERase-In (Ambion) was used as a Lysis buffer. The cell pellet was then lysed in the same volume of Lysis buffer on ice for 10 min. The nuclear membrane was disrupted by passage through a 28 G needle and then centrifuged at 14,000*g* for 15 min. Supernatants were collected as total cell extracts. After the protein concentration of cell extracts was adjusted to 5–8 mg/ml with Lysis buffer, cell extracts were mixed with agarose beads conjugated with anti-FLAG antibody (M2-agarose, Sigma) and incubated overnight at 4°C. After washing with Lysis buffer for three times, non-specific protein binding to the anti-FLAG agarose beads was washed out by incubating with FLAG peptide at 50 μg/ml for 15 min at 4°C. This step was critical to wash out non-specific or weak binding to the anti-FLAG agarose beads. To elute the protein complex with 3XFLAG-tagged protein, 3XFLAG peptides were added to the agarose beads at 500 μg/ml and incubated for 1 h at 4°C. Eluted proteins were then analysed by immunoblotting. For immunoprecipitation of HA-tagged protein, anti-HA-agarose (Sigma) was used instead of anti-FLAG agarose, and the precipitated proteins were eluted with SDS-sample buffer.

For immunoprecipitation of mature U snRNPs, a nuclear pellet was obtained from suspension cells using Buffer A (50 mM Hepes pH 7.5/1 mM $MgCl_2$/1 mM EGTA/1 mM DTT/protease inhibitors) on ice for 10 min followed by centrifugation at 3000*g* for 5 min. The nuclear pellet was lysed in Buffer A supplemented with 150 mM KCl, 1% NP-40, 10% glycerol, and RNase inhibitor SUPERase-In (Ambion) and then the nuclear membrane was disrupted by passage through a 27 G syringe 10 times and a repeated freeze/thaw cycle 3 times. Nuclear extract was obtained after the removal of cell debris by centrifugation at 20,000*g* for 10 min. Anti-Sm proteins monoclonal antibody (Y12) and mouse immunoglobulin (as negative control) were used for immunoprecipitation. Antibodies used for Western

The paper explained

PROBLEM:

The motor neuron diseases (ALS) and spinal muscular atrophy (SMA) are caused by dysfunction of proteins involved in RNA metabolism. For ALS, the RNA-binding proteins TDP-43 and FUS/TLS, have been implicated, while in SMA the protein SMN, essential for biogenesis of spliceosomal component snRNPs, is critical. A key question is whether there is a shared defective mechanism in RNA metabolism common to these two diseases.

RESULT:

We report a convergent function for TDP-43, FUS/TLS and SMN by showing that the genes for these diseases share a common mechanism: maintenance of nuclear Gems and controlling the level of U snRNA spliceosomal complex. In ALS spinal motor neurons as well as TDP-43 depleted neurons, we observed disruption of Gems and abnormal accumulation of U snRNAs/snRNPs. Together, our findings indicate that TDP-43, FUS/TLS and SMN are important for spliceosome integrity, and that collapse of the spliceosome is the critical mechanism that must underlie the neurodegenerative process in both ALS and SMA.

IMPACT:

Our study reveals the important role of nuclear Gems and spliceosomal U snRNPs in motor neuron survival. Although it requires more investigation, our work substantially contributes to understanding the molecular mechanism of motor neuron disease by providing evidence linking for the first time the selective vulnerability of motor neurons to spliceosome breakdown in Gems of ALS and SMA. Furthermore, targeting spliceosome and/or Gem stability in motor neurons may represent a new class of candidate therapeutics for motor neuron diseases.

blot were as follows: mouse anti-FUS/TLS (Santa Cruz, sc-47711), rat anti-PRPF3 (MBL, clone 4E3), goat anti-U1-70K (Santa Cruz), mouse anti-PABP (Sigma, clone 10E10) and rabbit anti-eIF4G (Cell Signaling, #2498).

FUS/TLS knockout mice

ES cell clone (HMA274) with β-Gal-neo cassette inserted between exon 2 and 3 of *FUS/TLS* gene were obtained from mutant mouse regional resource centers at University of California, Davis, and used to generate FUS/TLS heterozygous mice with support by Research Resource Center of RIKEN Brain Science Institute. Genotyping of mice with disrupted FUS/TLS allele was performed using RT-PCR, and FUS/TLS protein levels were confirmed by Western blot analysis. Heterozygote mice (F3) were intercrossed to generate $FUS^{-/-}$ mice.

Postmortem human tissues

Specimens of spinal cords from five patients with sporadic ALS and seven other neurological disease patients as controls, as well as temporal lobes from three patients with FTLD-TDP and four other neurological disease patients as controls, were obtained by autopsy with informed consent (Supporting Information Table S1). The diagnosis of ALS was confirmed by El Escorial diagnostic criteria as defined by the World Federation of Neurology and with the presence of TDP-43 pathology, as detected by histopathology. For the diagnosis of FTLD-TDP, selective sections were immunostained with antibodies against phosphorylated tau, ubiquitin, phosphorylated TDP-43 and FUS/TLS to select FTLD-TDP (Cairns et al, 2007). All patients with ALS and FTLD-TDP showed no hereditary traits. The collection of tissues and their use in this study was approved by the ethics committee of Nagoya University Graduate School of Medicine, Fukushimura Hospital, Tokyo Metropolitan Institute, and RIKEN. Tissues for RNA analysis were immediately frozen using liquid nitrogen and stored at −80°C until use. For immunofluorescent staining, 6 μm sections were prepared from paraffin-embedded tissues, deparaffinized, microwaved for 20 min in 50 mM citrate buffer (pH 6.0), treated with TNB blocking buffer (PerkinElmer, Boston, MA) and then incubated with primary antibodies. After washing, sections were incubated with Alexa-546-conjugated goat anti-rabbit IgG (1:1000; Invitrogen) and Alexa-488-conjugated goat anti-mouse IgG (1:1000; Invitrogen) for 30 min, mounted with Prolong gold antifade reagent (Invitrogen) and then imaged with a laser confocal microscope (LSM710, Carl Zeiss, Jena, Germany). The position of the nucleus was confirmed by TO-PRO-3 Iodidel (Invitorgen). For immunohistochemistry, sections were deparaffinized and boiled for 20 min in 50 mM citrate buffer (pH 6.0), treated with 3% goat serum/0.5% tween-20/PBS supplemented with Avidin solution (Vector, Avidin/Biotin Blocking kit, #SP-2001), and then incubated with primary antibodies in 3% goat serum/0.5% tween-20/PBS supplemented with Biotin solution (Vector, Avidin/Biotin Blocking kit). After washing, sections were incubated with Biotin-conjugated anti-mouse IgG or anti-rabbit IgG (1:400, Vector) in 0.05%Tween-20/PBS. Signals were visualized with Vectastain ABC kit (Elite, #PK-6100) and Metal Enhanced DAB substrate kit (Thermo Scientific, #34065).

Quantitative RT-PCR

Prior to RNA extraction, cultured cells were harvested and stored in RNAlater (Ambion), and frozen tissue samples were stored in RNAlater ICE (Ambion). Total RNA containing a small RNA fraction was extracted with a *mir*Vana miRNA Isolation Kit (Ambion) according to the manufacturer's instructions, and then treated with DNase (TURBO DNA-free Kit, Ambion) for either 20 min or 1 h depending on whether the source was cultured cells or tissue samples, respectively. U snRNAs were transcribed with specific primers as described previously (Zhang et al, 2008), and RNA levels were quantified with specific primers as described previously (Zhang et al, 2008) using the Syber Green system (Applied Biosystems). The primers we used are listed in Supporting

Information Table S3. All PCR reactions were performed in triplicate. RNA levels in samples were normalized with GAPDH for mRNA, and average of 5S and 5.8S for small RNA.

For more detailed Materials and Methods see the Supporting Information.

Author contributions

HT and KY designed the study; HT, YI, AF and AK performed the experiments; YI, HH, NA, FT, YH, HA, SM and GS obtained the patient autopsy samples and performed neuropathological and clinical diagnosis; HH and SM advised the staining of human sample; YI, NA, FT and GS provided critical inputs for the manuscript; HT analysed the data and KY provided inputs to analysis; HT and KY wrote the manuscript. All authors approved the manuscript.

Acknowledgements

The authors thank Prof. Haruhiko Siomi (Keio University) for a critical reading of manuscript and advice, and the Research Resource Center of RIKEN Brain Science Institute for their technical support with the Mass spectrometric analysis and generating FUS knockout mice. This work was supported by Grants-in-Aid nos. 23111006 and 23110523 (to KY) for Scientific Research on Innovative Areas, Comprehensive Brain Science Network for Scientific Research on Innovative Areas (to SM, HA), Grant-in-Aid no. 23700455 for Young Scientists (B) (to HT), from the Ministry for Education, Culture, and Sports, Science and Technology of Japan; by Grants-in-Aid (to KY, GS, SM) from the Research Committee of CNS Degenerative Diseases, the Ministry of Health, Labor and Welfare of Japan; and by Research Funding for Longevity Sciences (22-14) (to SM) from the National Center for Geriatrics and Gerontology, Japan.

Supporting Information is available at EMBO Molecular Medicine online.

The authors declare that they have no conflict of interest.

References

Andersen PM, Al-Chalabi A (2011) Clinical genetics of amyotrophic lateral sclerosis: what do we really know? Nat Rev Neurol 7: 603-615

Arai T, Hasegawa M, Akiyama H, Ikeda K, Nonaka T, Mori H, Mann D, Tsuchiya K, Yoshida M, Hashizume Y, *et al* (2006) TDP-43 is a component of ubiquitin-positive tau-negative inclusions in frontotemporal lobar degeneration and amyotrophic lateral sclerosis. Biochem Biophys Res Commun 351: 602-611

Ayala YM, De Conti L, Avendano-Vazquez SE, Dhir A, Romano M, D'Ambrogio A, Tollervey J, Ule J, Baralle M, Buratti E, *et al* (2011) TDP-43 regulates its mRNA levels through a negative feedback loop. EMBO J 30: 277-288

Berg MG, Singh LN, Younis I, Liu Q, Pinto AM, Kaida D, Zhang Z, Cho S, Sherrill-Mix S, Wan L *et al* (2012) U1 snRNP determines mRNA length and regulates isoform expression. Cell 150: 53-64

Blauw HM, Barnes CP, van Vught PW, van Rheenen W, Verheul M, Cuppen E, Veldink JH, van den Berg LH (2012) SMN1 gene duplications are associated with sporadic ALS. Neurology 78: 776-780

Bond CS, Fox AH (2009) Paraspeckles: nuclear bodies built on long noncoding RNA. J Cell Biol 186: 637-644

Boulisfane N, Choleza M, Rage F, Neel H, Soret J, Bordonne R (2011) Impaired minor tri-snRNP assembly generates differential splicing defects of U12-type introns in lymphoblasts derived from a type I SMA patient. Hum Mol Genet 20: 641-648

Buratti E, Dork T, Zuccato E, Pagani F, Romano M, Baralle FE (2001) Nuclear factor TDP-43 and SR proteins promote in vitro and in vivo CFTR exon 9 skipping. EMBO J 20: 1774-1784

Burghes AH, Beattie CE (2009) Spinal muscular atrophy: why do low levels of survival motor neuron protein make motor neurons sick? Nat Rev Neurosci 10: 597-609

Cairns NJ, Bigio EH, Mackenzie IR, Neumann M, Lee VM, Hatanpaa KJ, White CL III, Schneider JA, Grinberg LT, Halliday G, *et al* (2007) Neuropathologic diagnostic and nosologic criteria for frontotemporal lobar degeneration: consensus of the Consortium for Frontotemporal Lobar Degeneration. Acta Neuropathol 114: 5-22

Casafont I, Bengoechea R, Tapia O, Berciano MT, Lafarga M (2009) TDP-43 localizes in mRNA transcription and processing sites in mammalian neurons. J Struct Biol 167: 235-241

Chen-Plotkin AS, Lee VM, Trojanowski JQ (2010) TAR DNA-binding protein 43 in neurodegenerative disease. Nat Rev Neurol 6: 211-220

Cooper TA, Wan L, Dreyfuss G (2009) RNA and disease. Cell 136: 777-793

Coovert DD, Le TT, McAndrew PE, Strasswimmer J, Crawford TO, Mendell JR, Coulson SE, Androphy EJ, Prior TW, Burghes AH (1997) The survival motor neuron protein in spinal muscular atrophy. Hum Mol Genet 6: 1205-1214

Corcia P, Camu W, Halimi JM, Vourc'h P, Antar C, Vedrine S, Giraudeau B, de Toffol B, Andres CR (2006) SMN1 gene, but not SMN2, is a risk factor for sporadic ALS. Neurology 67: 1147-1150

D'Ambrogio A, Buratti E, Stuani C, Guarnaccia C, Romano M, Ayala YM, Baralle FE (2009) Functional mapping of the interaction between TDP-43 and hnRNP A2 in vivo. Nucleic Acids Res 37: 4116-4126

Dion PA, Daoud H, Rouleau GA (2009) Genetics of motor neuron disorders: new insights into pathogenic mechanisms. Nat Rev Genet 10: 769-782

Ebert AD, Yu J, Rose FF, Jr, Mattis VB, Lorson CL, Thomson JA, Svendsen CN (2009) Induced pluripotent stem cells from a spinal muscular atrophy patient. Nature 457: 277-280

Fiesel FC, Voigt A, Weber SS, Van den Haute C, Waldenmaier A, Gorner K, Walter M, Anderson ML, Kern JV, Rasse TM, *et al* (2010) Knockdown of transactive response DNA-binding protein (TDP-43) downregulates histone deacetylase 6. EMBO J 29: 209-221

Gabanella F, Butchbach ME, Saieva L, Carissimi C, Burghes AH, Pellizzoni L (2007) Ribonucleoprotein assembly defects correlate with spinal muscular atrophy severity and preferentially affect a subset of spliceosomal snRNPs. PLoS One 2: e921

Giesemann T, Rathke-Hartlieb S, Rothkegel M, Bartsch JW, Buchmeier S, Jockusch BM, Jockusch H (1999) A role for polyproline motifs in the spinal muscular atrophy protein SMN. Profilins bind to and colocalize with smn in nuclear gems. J Biol Chem 274: 37908-37914

Huang J, Furuya A, Furuichi T (2007) Very-KIND, a KIND domain containing RasGEF, controls dendrite growth by linking Ras small GTPases and MAP2. J Cell Biol 179: 539-552

Kariya S, Re DB, Jacquier A, Nelson K, Przedborski S, Monani UR (2012) Mutant superoxide dismutase 1 (SOD1), a cause of amyotrophic lateral sclerosis, disrupts the recruitment of SMN, the spinal muscular atrophy protein to nuclear Cajal bodies. Hum Mol Genet 21: 3421-3434

Kolb SJ, Battle DJ, Dreyfuss G (2007) Molecular functions of the SMN complex. J Child Neurol 22: 990-994

Kumaran RI, Thakar R, Spector DL (2008) Chromatin dynamics and gene positioning. Cell 132: 929-934

Lagier-Tourenne C, Cleveland DW (2009) Rethinking ALS: the FUS about TDP-43. Cell 136: 1001-1004

Lee EB, Lee VM, Trojanowski JQ (2012) Gains or losses: molecular mechanisms of TDP43-mediated neurodegeneration. Nat Rev Neurosci 13: 38-50

Lemmens R, Moore MJ, Al-Chalabi A, Brown RH, Jr, Robberecht W (2010) RNA metabolism and the pathogenesis of motor neuron diseases. Trends Neurosci 33: 249-258

Mao YS, Zhang B, Spector DL (2011) Biogenesis and function of nuclear bodies. Trends Genet 27: 295-306

Neumann M, Sampathu DM, Kwong LK, Truax AC, Micsenyi MC, Chou TT, Bruce J, Schuck T, Grossman M, Clark CM, *et al* (2006) Ubiquitinated TDP-43 in frontotemporal lobar degeneration and amyotrophic lateral sclerosis. Science 314: 130-133

Okuda T, Hattori H, Takeuchi S, Shimizu J, Ueda H, Palvimo JJ, Kanazawa I, Kawano H, Nakagawa M, Okazawa H (2003) PQBP-1 transgenic mice show a late-onset motor neuron disease-like phenotype. Hum Mol Genet 12: 711-725

Pellizzoni L, Yong J, Dreyfuss G (2002) Essential role for the SMN complex in the specificity of snRNP assembly. Science 298: 1775-1779

Polymenidou M, Lagier-Tourenne C, Hutt KR, Huelga SC, Moran J, Liang TY, Ling SC, Sun E, Wancewicz E, Mazur C, *et al* (2011) Long pre-mRNA depletion and RNA missplicing contribute to neuronal vulnerability from loss of TDP-43. Nat Neurosci 14: 459-468

Rabin SJ, Kim JM, Baughn M, Libby RT, Kim YJ, Fan Y, La Spada A, Stone B, Ravits J (2010) Sporadic ALS has compartment-specific aberrant exon splicing and altered cell-matrix adhesion biology. Hum Mol Genet 19: 313-328

Sephton CF, Cenik C, Kucukural A, Dammer EB, Cenik B, Han Y, Dewey CM, Roth FP, Herz J, Peng J, *et al* (2011) Identification of neuronal RNA targets of TDP-43-containing ribonucleoprotein complexes. J Biol Chem 286: 1204-1215

Shan X, Chiang PM, Price DL, Wong PC (2010) Altered distributions of Gemini of coiled bodies and mitochondria in motor neurons of TDP-43 transgenic mice. Proc Natl Acad Sci USA 107: 16325-16330

Talbot K, Davies KE (2008) Is good housekeeping the key to motor neuron survival? Cell 133: 572-574

Tollervey JR, Curk T, Rogelj B, Briese M, Cereda M, Kayikci M, Konig J, Hortobagyi T, Nishimura AL, Zupunski V, *et al* (2011) Characterizing the RNA targets and position-dependent splicing regulation by TDP-43. Nat Neurosci 14: 452-458

Tripsianes K, Madl T, Machyna M, Fessas D, Englbrecht C, Fischer U, Neugebauer KM, Sattler M (2011) Structural basis for dimethylarginine recognition by the Tudor domains of human SMN and SPF30 proteins. Nat Struct Mol Biol 18: 1414-1420

Ule J (2008) Ribonucleoprotein complexes in neurologic diseases. Curr Opin Neurobiol 18: 516-523

Veldink JH, Kalmijn S, Van der Hout AH, Lemmink HH, Groeneveld GJ, Lummen C, Scheffer H, Wokke JH, Van den Berg LH (2005) SMN genotypes producing less SMN protein increase susceptibility to and severity of sporadic ALS. Neurology 65: 820-825

Veldink JH, van den Berg LH, Cobben JM, Stulp RP, De Jong JM, Vogels OJ, Baas F, Wokke JH, Scheffer H (2001) Homozygous deletion of the survival motor neuron 2 gene is a prognostic factor in sporadic ALS. Neurology 56: 749-752

Wahl MC, Will CL, Luhrmann R (2009) The spliceosome: design principles of a dynamic RNP machine. Cell 136: 701-718

Wan L, Battle DJ, Yong J, Gubitz AK, Kolb SJ, Wang J, Dreyfuss G (2005) The survival of motor neurons protein determines the capacity for snRNP assembly: biochemical deficiency in spinal muscular atrophy. Mol Cell Biol 25: 5543-5551

Wang IF, Reddy NM, Shen CK (2002) Higher order arrangement of the eukaryotic nuclear bodies. Proc Natl Acad Sci USA 99: 13583-13588

Waragai M, Junn E, Kajikawa M, Takeuchi S, Kanazawa I, Shibata M, Mouradian MM, Okazawa H (2000) PQBP-1/Npw38, a nuclear protein binding to the polyglutamine tract, interacts with U5-15kD/dim1p via the carboxyl-terminal domain. Biochem Biophys Res Commun 273: 592-595

Wu CH, Fallini C, Ticozzi N, Keagle PJ, Sapp PC, Piotrowska K, Lowe P, Koppers M, McKenna-Yasek D, Baron DM, *et al* (2012) Mutations in the profilin 1 gene cause familial amyotrophic lateral sclerosis. Nature 488: 499-503

Xiao S, Sanelli T, Dib S, Sheps D, Findlater J, Bilbao J, Keith J, Zinman L, Rogaeva E, Robertson J (2011) RNA targets of TDP-43 identified by UV-CLIP are deregulated in ALS. Mol Cell Neurosci 47: 167-180

Yamazaki T, Chen S, Yu Y, Yan B, Haertlein TC, Carrasco MA, Tapia JC, Zhai B, Das R, Lalancette-Hebert M, *et al* (2012) FUS-SMN protein interactions link the motor neuron diseases ALS and SMA. Cell Rep 2: 799-806

Zhang Z, Lotti F, Dittmar K, Younis I, Wan L, Kasim M, Dreyfuss G (2008) SMN deficiency causes tissue-specific perturbations in the repertoire of snRNAs and widespread defects in splicing. Cell 133: 585-600

Neurobiology of Aging 34 (2013) 1101–1104

Contents lists available at SciVerse ScienceDirect

Neurobiology of Aging

journal homepage: www.elsevier.com/locate/neuaging

Brief communication

Suspected limited efficacy of γ-secretase modulators

Nobuto Kakuda [a,b], Kohei Akazawa [c], Hiroyuki Hatsuta [d], Shigeo Murayama [d], Yasuo Ihara [a,b,e,f,*], The Japanese Alzheimer's Disease Neuroimaging Initiative

[a] Department of Neuropathology, Faculty of Life and Medical Sciences, Doshisha University, Kyoto, Japan
[b] Core Research for Evolutional Science and Technology (CREST), Japan Science and Technology Agency, Saitama, Japan
[c] Department of Medical Informatics, Niigata University Medical and Dental Hospital, Niigata University, Niigata, Japan
[d] Department of Neuropathology, Tokyo Metropolitan Institute of Gerontology, Tokyo, Japan
[e] Center for Neurologic Diseases, Doshisha University, Kyoto, Japan
[f] New Energy and Industrial Technology Development Organization (NEDO), Kanagawa, Japan

ARTICLE INFO

Article history:
Received 16 June 2012
Accepted 25 August 2012
Available online 9 October 2012

Keywords:
γ-Secretase
γ-Modulator
Alzheimer's disease

ABSTRACT

Mild cognitive impairment and Alzheimer's disease (AD) are associated with changes in γ-secretase activity in the brain, producing an amyloid β-protein-42-lowering γ-modulator-like effect. We show here that this modulation occurs at the stage of amyloid deposition, presumably decades earlier than the onset of AD. In addition, γ-secretase modulator-1, a γ-modulator, altered γ-secretase activity in the AD brain but to a lesser extent than in the normal brain. These findings suggest that γ-modulators have limited efficacy against amyloid deposition and AD.

1. Introduction

Amyloid β-protein (Aβ) is cleaved sequentially from amyloid precursor protein by β- and γ-secretases (for a review see Selkoe, 2001). The longer but minor species, Aβ42, predominates in senile plaques (Iwatsubo et al., 1994). γ-Secretase, a heterogeneous complex (Takasugi et al., 2003; Serneels et al., 2009), governs the intramembrane proteolysis of type I membrane proteins including amyloid precursor protein (Sisodia and St George-Hyslop, 2002; Wakabayashi and De Strooper, 2008). We found recently that γ-secretase activity is altered in brains affected by mild cognitive impairment (MCI) or Alzheimer's disease (AD). The change decreases the concentrations of both Aβ42 and Aβ43 in cerebrospinal fluid (CSF) in patients affected with MCI or AD. To compensate for these decreases, the levels of Aβ38 and Aβ40 are increased (Kakuda et al., 2012). We assume that Aβ42 and Aβ43 are enhanced to be converted by stepwise processing to Aβ38 and Aβ40, respectively, by altered γ-secretase in the brain affected by MCI or AD (Kakuda et al., 2012; Takami et al., 2009). Reciprocal changes in the levels of Aβ42 and Aβ38 without a change in the total Aβ level are an essential characteristic of γ-secretase modulators, drugs whose development receives intense attention.

2. Materials and methods

2.1. Subjects

Human cortical specimens for quantification of raft-associated γ-secretase activity were obtained from brains that had been removed, processed, and stored at −80 °C within 12 hours postmortem; the bodies had been placed in a cold (4 °C) room within 2 hours after death. The specimens were kept at the Brain Bank at Tokyo Metropolitan Institute of Gerontology. For all the brains registered at the bank we obtained written informed consent for their use for medical research from the patient or the patient's family. Each brain specimen (approximately 0.5 g) was taken from Brodmann areas 9–11 of 13 AD patients (80 ± 5.0 years of age; Braak neurofibrillary tangle [NFT] stage >IV; senile plaque [SP] stage = C; retrospective clinical dementia rating [CDR] >1), 10 SP stage B patients (76 ± 4.0 years of age; Braak NFT stage >I; retrospective CDR = 0), 10 SP stage A patients (76 ± 4.7 years of age; Braak NFT stage >0; retrospective CDR = 0), and 16 controls in SP stage 0 (77 ± 6.5 years of age; Braak NFT stage <I; retrospective CDR = 0). SP stages were determined by modified methenamine silver stain: stage A: Aβ deposits in the basal portions of the isocortex; stage B: Aβ deposits in virtually all isocortical association

* Corresponding author at: Department of Neuropathology, Faculty of Life and Medical Sciences, Doshisha University, 4-1-1, Kizugawadai, Kizugawa, Kyoto 619-0225, Japan. Tel.: +81 774 65 6058; fax: +81 3 5800 6852.
E-mail address: yihara@mail.doshisha.ac.jp (Y. Ihara).

0197-4580/$ – see front matter © 2013 Elsevier Inc. All rights reserved.
http://dx.doi.org/10.1016/j.neurobiolaging.2012.08.017

areas except primary centers; stage C (AD): Aβ deposits in all areas of the isocortex including primary motor and sensory centers (Braak and Braak, 1991).

2.2. Quantification of brain raft-associated γ-secretase activity

A previously reported assay method was employed with some modifications (Kakuda et al., 2012). Briefly, each raft fraction, adjusted to 100 μg/mL in protein concentration, was incubated with 200 nM of βCTF-FLAG for 1 hour at 37 °C in the presence of 0, or 0.1–0.5 μM γ-secretase modulator (GSM)-1 (kindly provided by Dr M. Okochi, Osaka University). After incubation, all samples were centrifuged at 265,000*g* on a TLA110 rotor (Beckman, Palo Alto, CA, USA) for 20 minutes at 4 °C. The supernatants were separated on sodium dodecyl sulfate polyacylamide gel electrophoresis (SDS-PAGE), and subjected to quantitative Western blot analysis, using specific antibodies, 3B1 for Aβ38, BA27 for Aβ40, 44A3 for Aβ42, and anti-Aβ43 polyclonal for Aβ43.

2.3. GSM-1-induced shift of ln(Aβ38/42)

Shifts of ln(Aβ38/42) with GSM-1 were calculated as GSM-1-induced ln(Aβ38/42) minus the ratio measured in its absence.

2.4. Statistical analysis

All statistical analyses were performed using SPSS version 14.0. Data transformation was required to achieve normal distributions; all analyses were performed after logarithmic transformation of the data for Aβ38, Aβ40, Aβ42, and Aβ43. Analysis of variance was used to test the equality of mean values for continuous variables between the 4 groups: control, SP stage A, SP stage B, and AD. Multiple comparisons were made using Bonferroni *t* test to test the differences between controls, SP stage A, SP stage B, and AD. The paired *t* test was used to examine the effect of GSM-1 treatment. *p* values <0.05 were considered significant.

3. Results

We speculated that this modulation in the γ-secretase activity occurs much earlier than the onset of AD because lower Aβ42 concentrations in CSF appear to be associated with amyloid deposition itself (Fagan et al., 2006). To confirm this, we measured the activities of raft-associated γ-secretase prepared from autopsied brains using a previously established method (Kakuda et al., 2012). Raft fractions were prepared from control and AD brains (Brodmann areas 9–11), which were judged histochemically to be in the Braak SP stage 0, stage A, stage B, or stage C (AD) (Braak and Braak, 1991). Aβs produced by γ-secretase from each brain specimen were analyzed by quantitative Western blot, and the ln(Aβ40/43) and ln(Aβ38/42) ratios were obtained. Stage A plots nearly superimposed with control plots (Fig. 1; 0 vs. A: $p = 1.000$ for ln(Aβ40/43), $p = 1.000$ for ln(Aβ38/42)). However, the γ-secretase activities differed between stage B specimens and 0/A specimens (0 vs. B: $p = 0.005$ for ln(Aβ40/43) and $p < 0.001$ for ln(Aβ38/42); A vs. B: $p = 0.002$ for ln(Aβ40/43) and $p = 0.001$ for ln(Aβ38/42); Fig. 1). AD (stage C) plots were shifted the most (0 vs. C: $p < 0.001$ for ln(Aβ40/43) and $p = 0.003$ for ln(Aβ38/42); A vs. C: $p < 0.001$ for ln(Aβ40/43) and $p = 0.007$ for ln(Aβ38/42)). Most interestingly, although AD plots were shifted to the same extent as stage B plots for Aβ38/42 (B vs. C: $p = 1.000$ for ln(Aβ38/42)), stage B and AD plots differ for Aβ40/43 (B vs. C: $p < 0.001$ for ln(Aβ40/43); Fig. 1).

Although these data were obtained from a cross-sectional study, one might assume that stage A develops through to stage B and eventually to stage C over decades (Duyckaerts and Hauw, 1997).

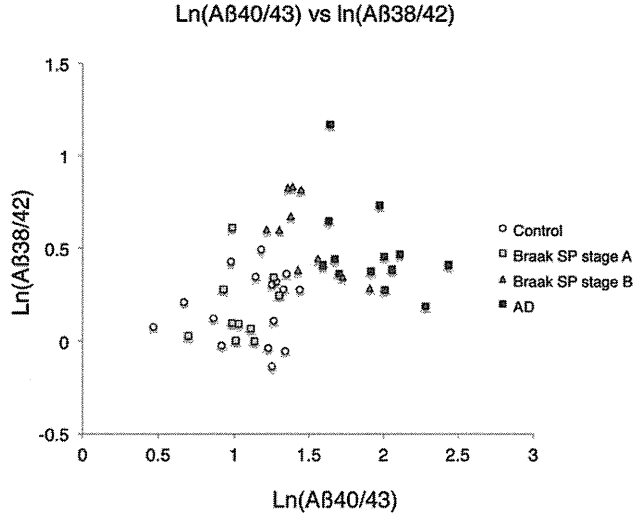

Fig. 1. Ln(amyloid-β protein [Aβ]40/43) versus ln(Aβ38/42) plot of raft-associated γ-secretase prepared from the brains in various (Braak) senile plaque (SP) stages. The raft-associated γ-secretase prepared from Braak SP stages 0, A, B, and C (AD) brain specimens were incubated with 200 nM of βCTF for 1 hour at 37 °C. After centrifugation of the reaction mixtures, the supernatants were saved for quantitative Western blot analysis of Aβs using specific antibodies.

Thus, the Aβ42 product line of γ-secretase appears to undergo changes early and the Aβ42-lowering activity remains constant through to development of AD. By contrast, the Aβ40 product line gradually changes with increasing Aβ40/43 ratio, as stage 0/A develops to stage B and finally to AD. Our previous observations showed that Aβ42 levels in CSF parallel the Aβ38/42 ratio, and Aβ43 levels parallel the Aβ40/43 ratio (Kakuda et al., 2012). These findings suggest that a decrease in the Aβ42 level would be the first alteration observable in CSF and that the level does not change throughout the disease course, whereas the Aβ43 level in CSF would decrease progressively up to AD.

We noted previously that the effects of Aβ42-lowering γ-modulators could be minimal in sporadic MCI/AD patients because modulation of γ-secretase has already begun in their brains. As mentioned above, the modulation of γ-secretase is evident in stage B. Accordingly, we investigated the response of γ-secretase to GSM-1, an Aβ42-lowering modulator, in control and AD brains. We reasoned that a strong response of the altered γ-secretase to GSM-1 would indicate that the drug might still be effective.

We quantified γ-secretase activities in the absence or presence of GSM-1 in control and AD specimens. This agent is known to aggressively modulate only conversion from Aβ42 to Aβ38, but not that from Aβ43 to Aβ40 (Crump et al., 2011; Ebke et al., 2011; Ohki et al., 2011). As expected, GSM-1 treatment significantly lowered Aβ42 and increased Aβ38 in control (see Supplementary Fig. 1). By contrast, in AD specimens, GSM-1 lowered Aβ42 and increased Aβ38 but to a lesser extent (Supplementary Fig. 1). The generation of Aβ40 and Aβ43, and the total production of Aβ were unchanged by the treatment of GSM-1 in all specimens (Supplementary Fig. 1).

In AD specimens, conversion of Aβ43 to Aβ40 seems to be altered compared with control (Kakuda et al., 2012), but this might be due to high concentrations of GSM-1 (>0.5 μM), which suppressed Aβ40 (and Aβ43) product line and total Aβ production in both control and AD specimens (data not shown). GSM-1 treatment significantly elevated the ratio of Aβ38/42 in control (Aβ38/42 with dimethyl sulfoxide vs. Aβ38/42 with GSM-1; $p < 0.000$, paired *t* test; Fig. 2A). By contrast, the same treatment of AD specimens

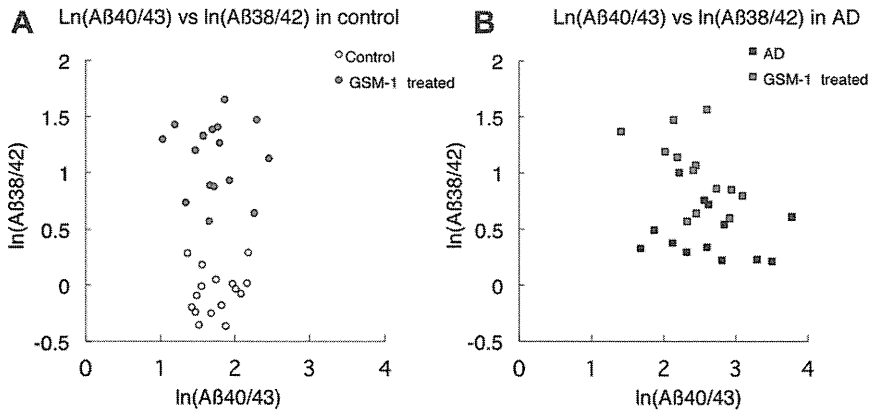

Fig. 2. Ln(amyloid-β protein [Aβ]40/43) versus ln(Aβ38/42) plot of γ-secretase modulator (GSM)-1-treated raft-associated γ-secretase activity. The raft-associated γ-secretases prepared from control (A) and AD (B) brains were incubated with 200 nM of βCTF for 1 hour at 37 °C in the presence of dimethyl sulfoxide or 0.3 μM GSM-1. Aβs produced were quantified by quantitative Western blot analysis using specific antibodies.

caused a much smaller increase in the Aβ38/42 ratio ($p < 0.001$ for AD paired t test; Fig. 2B). There was no significant difference in the Aβ40/43 ratio between control and AD specimens (Aβ40/43 with dimethyl sulfoxide vs. Aβ40/43 with GSM-1; $p = 0.814$ for control; $p = 0.223$ for AD, respectively; paired t test; Fig. 2A and B). The modulating effect on the Aβ38/42 ratio can be interpreted as indicating the extent of GSM-1-induced shift in the Aβ38/42 ratio (Supplementary Table 1). γ-Secretase was associated with significantly lower ratios in AD specimens than in control specimens (control vs. AD: $p < 0.001$), indicating a poor response to GSM-1 in AD specimens.

4. Discussion

Modulation of γ-secretase occurs in AD brains (Kakuda et al., 2012), and to a significant extent already at the stage of amyloid deposition, a decade or even decades before the onset of AD (Duyckaerts and Hauw, 1997). Although γ-secretase self-modulates and produces less Aβ42, it is likely that β-amyloid accumulation slowly progresses and ultimately extends throughout the brain, finally involving primary cortical centers (Duyckaerts and Hauw, 1997). A gradual decline in the rate of Aβ accumulation curve (Kawarabayashi et al., 2001) might be caused by self-modulation of γ-secretase. Currently, we do not know which comes first, Aβ deposition or γ-self-modulation. However, the efficacy of GSM-1 and γ-modulators in general would be limited when Aβ42 deposition and self-modulation of γ-secretase begins in the brain. To date, the efficacy of γ-modulators has been confirmed most often using younger Tg2576 mice, which do not yet accumulate Aβ (Borgegard et al., 2012; Kounnas et al., 2010). In Tg2576 mice, Aβ deposition starts at 9–12 months, and γ-secretase activity changes together with increasing Aβ deposition in the brain starting at 15–16 months of age (Kawarabayashi et al., 2001; data not shown). Thus, the true effectiveness of γ-modulators in Tg2576 mice should be assessed after 15–16 months of age. It is unclear whether γ-modulators are effective in such amyloid-bearing aged mice.

Disclosure statement

The authors have no conflict of interest.

Ethic permission was approved by Faculty of Life and Medical Sciences, Doshisha University, and we obtained written informed consent for their use for medical research from the patient or the patient's family.

Acknowledgements

The authors thank Dr Masayasu Okochi, Neuropsychiatry and Neurochemistry, Department of Integrated Medicine, Osaka University Graduate School of Medicine, for kindly providing GSM-1, and Dr Satoru Funamoto, Department of Neuropathology, Faculty of Life and Medical Sciences, Doshisha University, for providing βCTF. This project was supported in part by the New Energy and Industrial Technology Development Organization, Japan (J-ADNI) and by the MEXT-Supported Program for the Strategic Research Foundation at Private Universities, 2012–2017.

Appendix A. Supplementary data

Supplementary data associated with this article can be found, in the online version, at http://dx.doi.org/10.1016/j.neurobiolaging.2012.08.017.

References

Borgegard, T., Juréus, A., Olsson, F., Rosqvist, S., Sabirsh, A., Rotticci, D., Paulsen, K., Klintenberg, R., Yan, H., Waldman, M., Stromberg, K., Nord, J., Johansson, J., Regner, A., Parpal, S., Malinowsky, D., Radesater, A.C., Li, T., Singh, R., Eriksson, H., Lundkvist, J., 2012. First and second generation γ-secretase modulators (GSMs) modulate amyloid-β (Aβ) peptide production through different mechanisms. J. Biol. Chem. 287, 11810–11819.

Braak, H., Braak, E., 1991. Neuropathological stageing of Alzheimer-related changes. Acta Neuropathol. 82, 239–259.

Crump, C.J., Fish, B.A., Castro, S.V., Chau, D.M., Gertsik, N., Ahn, K., Stiff, C., Pozdnyakov, N., Bales, K.R., Johnson, D.S., Li, Y.M., 2011. Piperidine acetic acid based γ-secretase modulators directly bind to Presenilin-1. ACS Chem. Neurosci. 2, 705–710.

Duyckaerts, C., Hauw, J.J., 1997. Prevalence, incidence and duration of Braak's stages in the general population: can we know? Neurobiol. Aging 18, 362–369.

Ebke, A., Luebbers, T., Fukumori, A., Shirotani, K., Haass, C., Baumann, K., Steiner, H., 2011. Novel γ-secretase enzyme modulators directly target presenilin protein. J. Biol. Chem. 286, 37181–37186.

Fagan, A.M., Mintun, M.A., Mach, R.H., Lee, S.Y., Dence, C.S., Shah, A.R., LaRossa, G.N., Spinner, M.L., Klunk, W.E., Mathis, C.A., DeKosky, S.T., Morris, J.C., Holtzman, D.M., 2006. Inverse relation between in vivo amyloid imaging load and cerebrospinal fluid Abeta42 in humans. Ann. Neurol. 59, 512–519.

Iwatsubo, T., Odaka, A., Suzuki, N., Mizusawa, H., Nukina, N., Ihara, Y., 1994. Visualization of Aβ42(43) and Aβ40 in senile plaque with end-specific Aβ monoclonals: evidence that an initially deposited forms is Aβ42(43). Neuron 13, 45–53.

Kakuda, N., Shoji, M., Arai, H., Furukawa, K., Ikeuchi, T., Akazawa, K., Takami, M., Hatsuta, H., Murayama, S., Hashimoto, Y., Miyajima, M., Arai, H., Nagashima, Y., Yamaguchi, H., Kuwano, R., Nagaike, K., Ihara, Y., Japanese Alzheimer's Disease Neuroimaging Initiative, 2012. Altered γ-secretase activity in mild cognitive impairment and Alzheimer's disease. EMBO Mol. Med. 4, 344–352.

Kawarabayashi, T., Younkin, L.H., Saido, T.C., Shoji, M., Ashe, K.H., Younkin, S.G., 2001. Age-dependent changes in brain, CSF, and plasma amyloid (β) protein in the Tg2576 transgenic mouse model of Alzheimer's disease. J. Neurosci. 21, 372–381.

Kounnas, M.Z., Danks, A.M., Cheng, S., Tyree, C., Ackerman, E., Zhang, X., Ahn, K., Nguyen, P., Comer, D., Mao, L., Yu, C., Pleynet, D., Digregorio, P.J., Velicelebi, G., Stauderman, K.A., Comer, W.T., Mobley, W.C., Li, Y.M., Sisodia, S.S., Tanzi, R.E., Wagner, S.L., 2010. Modulation of gamma-secretase reduces beta-amyloid deposition in a transgenic mouse model of Alzheimer's disease. Neuron 67, 769–780.

Ohki, Y., Higo, T., Uemura, K., Shimada, N., Osawa, S., Berezovska, O., Yokoshima, S., Fukuyama, T., Tomita, T., Iwatsubo, T., 2011. Phenylpiperidine-type γ-secretase modulators target the transmembrane domain 1 of presenilin 1. EMBO J. 30, 4815–4824.

Selkoe, D.J., 2001. Alzheimer's disease: genes, proteins, and therapy. Physiol. Rev. 81, 741–766.

Serneels, L., Van Biervliet, J., Craessaerts, K., Dejaegere, T., Horré, K., Van Houtvin, T., Esselmann, H., Paul, S., Schäfer, M.K., Berezovska, O., Hyman, B.T., Sprangers, B., Sciot, R., Moons, L., Jucker, M., Yang, Z., May, P.C., Karran, E., Wiltfang, J., D'Hooge, R., De Strooper, B., 2009. γ-Secretase heterogeneity in the Aph1 subunit: relevance for Alzheimer's disease. Science 324, 639–642.

Sisodia, S.S., St George-Hyslop, P.H., 2002. gamma-Secretase, Notch, Abeta and Alzheimer's disease: where do the presenilins fit in? Nat. Rev. Neurosci. 3, 281–290.

Takami, M., Nagashima, Y., Sano, Y., Ishihara, S., Morishima-Kawashima, M., Funamoto, S., Ihara, Y., 2009. γ-Secretase: successive tripeptide and tetrapeptide release from the transmembrane domain of β-carboxyl terminal fragment. J. Neurosci. 29, 13042–13052.

Takasugi, N., Tomita, T., Hayashi, I., Tsuruoka, M., Niimura, M., Takahashi, Y., Thinakaran, G., Iwatsubo, T., 2003. The role of presenilin cofactors in the γ-secretase complex. Nature 422, 438–441.

Wakabayashi, T., De Strooper, B., 2008. Presenilins: members of the gamma-secretase quartets, but part-time soloists too. J. Physiol. 23, 194–204.

Environmental Characteristics and Oxidative Stress of Inhabitants and Patients with Amyotrophic Lateral Sclerosis in a High-incidence Area on the Kii Peninsula, Japan

Tameko Kihira, Kazushi Okamoto, Sohei Yoshida, Tetuya Kondo, Keiko Iwai, Sachiko Wada, Yoshinori Kajimoto, Tomoyoshi Kondo, Yasumasa Kokubo and Shigeki Kuzuhara

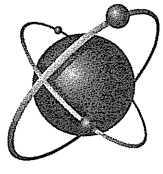

INTERNAL MEDICINE

Reprinted from Internal Medicine
Vol. 52, Pages 1479-1486
July 2013

INTERNAL MEDICINE

□ ORIGINAL ARTICLE □

Environmental Characteristics and Oxidative Stress of Inhabitants and Patients with Amyotrophic Lateral Sclerosis in a High-incidence Area on the Kii Peninsula, Japan

Tameko Kihira[1], Kazushi Okamoto[2], Sohei Yoshida[1], Tetuya Kondo[1], Keiko Iwai[3], Sachiko Wada[3], Yoshinori Kajimoto[4], Tomoyoshi Kondo[4], Yasumasa Kokubo[5] and Shigeki Kuzuhara[5,6]

Abstract

Objective Although Oshima, in the Kii Peninsula of Japan, is located within a high incidence area of amyotrophic lateral sclerosis (ALS) (Koza/Kozagawa/Kushimoto area, K area), no patients with ALS were detected between 1960 and 1999. However, the incidence recently increased between 2000 and 2009. On Oshima, the source of drinking water was changed from a regional river/wells to the Kozagawa River in the K area in 1975. We speculate that this change in water source may have played a role in the recent increase in the incidence of ALS. The aim of this study is to find contributing factors that may have triggered the locally high incidence of ALS.

Methods We investigated a possible association between the mineral content of drinking water and serum and oxidative stress markers among patients with ALS in the K area (K-ALS), residents of Oshima and controls.

Results We found that the levels of Ca and Zn in the recent drinking water in Oshima are low and that the serum levels of Ca and Zn in the Oshima residents and patients with K-ALS were significantly lower, while the oxidative stress markers were significantly higher, than those of the controls. The serum Zn and urinary 8-OHdG/creatinine levels explained 60% and 58% of the variations among the three groups, respectively. The serum Zn levels were negatively correlated with the serum Cu levels in the patients with K-ALS, and the serum Cu levels exhibited a tendency to be positively correlated with the 8-OHdG/creatinine levels in both the patients with K-ALS (r: 0.64) and the residents free from K-ALS (r: 0.32, $p<0.01$).

Conclusion Taken together, we suggest that the low levels of Ca and Zn in the drinking water are possibly associated with an imbalance of metal metabolism in Oshima residents and an increase in oxidative stress markers in patients with K-ALS, although the causative relationship is not clear. This is a cross-sectional study, and a prospective study is needed in the future.

Key words: focus area, environment, Kii-ALS, Cu/Zn, 8-OHdG

(Intern Med 52: 1479-1486, 2013)
(DOI: 10.2169/internalmedicine.52.9521)

[1]Department of Health Sciences, Kansai University of Health Sciences, Japan, [2]Department of Public Health, Aichi Prefectural University, Japan, [3]Faculty of Nursing, Kansai University of Health Sciences, Japan, [4]Department of Neurology, Wakayama Medical University, Japan, [5]Department of Neurology, Mie University Graduate School of Medicine, Japan and [6]Department of Medical Welfare, Suzuka University of Medical Science, Japan

Received for publication December 13, 2012; Accepted for publication February 25, 2013

Correspondence to Dr. Tameko Kihira, tkihira815@kansai.ac.jp

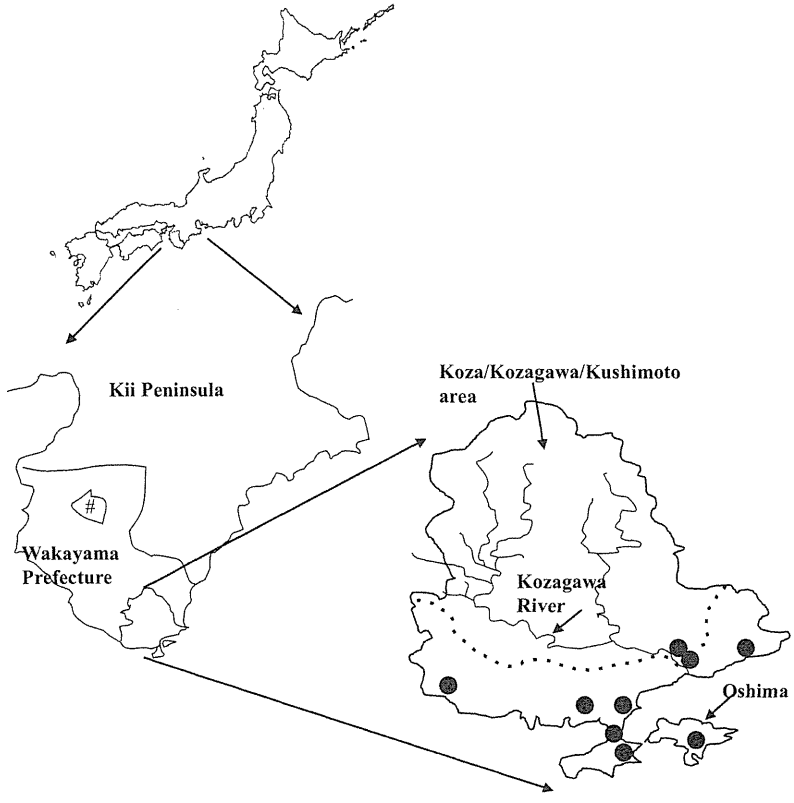

Figure 1. Geography of the Koza/Kozagawa/Kushimoto area and Oshima and the distribution of patients with ALS. The Koza/Kozagawa/Kushimoto (K) area is located in the southern part of the Kii peninsula of Japan. Oshima is included in the K area and is an island opposite to the mainland K area.The control area (#) is located in the northern part of the Kii peninsula. ALS patients in the K area detected between 2000 and 2009 who participated in the present research are shown. ●: a patient with ALS

Introduction

Amyotrophic lateral sclerosis (ALS) is a lethal, devastating adult-onset degenerative disease of the upper and lower motor neuron systems of unknown etiology. Many mechanisms have been postulated in the pathogenesis of ALS, including oxidative stress, accumulation of intracellular aggregates, mitochondrial damage, dysfunction in axonal transport, growth factor deficiency, aberrant RNA metabolism, glial cell pathology and Ca-induced excitotoxicity, and it is strongly suggested that interactions between environmental factors and genetic factors are involved in the development of ALS (1, 2). The Koza/Kozagawa/Kushimoto (K) area (the southern part of the Kii Peninsula) of Japan exhibited a 10-fold higher incidence of ALS compared to other areas of the world in the 1950s and 1960s, as did Guam (3-6). Then, the incidence gradually decreased, and the high incidence focus disappeared in Guam in the 1980s (7). However, the incidence of ALS in the K area recently increased to two- to three-fold higher than that observed in other areas (8, 9). On Oshima, a small island opposite the mainland K area, where the source of drinking water was changed from a regional river, wells and rainfall to the Kozagawa River in the mainland K area in 1975, we found three patients with ALS after 2000 despite the lack of patients with ALS between 1960 and 1999. The basin area from the Kozagawa River has been reported to be a high-incidence area of ALS in the 1950s and 1960s (5, 10, 11). We speculate that the change in water source may consequently have played a role in the appearance of new ALS patients in this area. Aiming to find contributing factors that may have triggered the locally high incidence of ALS, we cross-sectionally investigated a possible association between the drinking water mineral content and the serum mineral levels in residents and patients with ALS in the K area, with special reference to oxidative stress markers.

Materials and Methods

Area of investigation

The Kii Peninsula is located in the central southern part of the Japanese mainland (Fig. 1). Wakayama Prefecture

Table 1. Levels of Minerals in the Water on Oshima, the Mainland K Area and the Control Areas

Drinking water	Oshima (n: 3)	The mainland K area (n: 4)	Control (n: 3)
Ca (mg/mL)	2.97 ± 0.06 *	4.20±0.56 *	14.97±5.58
Mg (mg/mL)	1.10± 0.00	1.53 ±0.54	1.90 ±0.76
Cu (mg/mL)	0.013 ± 0.006	0.025 ±0.024	0.023 ±0.006
Zn (mg/mL)	0.009 ± 0.007	0.013 ±0.02	0.012 ±0.008
Fe (mg/mL)	< 0.03	< 0.03	< 0.03

River water	Oshima	The mainland K area	Control
Ca (mg/mL)	10.7	2.4	8.6
Mg (mg/mL)	5.5	1.1	1.2
Cu (mg/mL)	< 0.01	< 0.01	< 0.01
Zn (mg/mL)	0.12	< 0.005	< 0.005
Fe (mg/mL)	0.26	< 0.03	< 0.03

Well water	Oshima	The mainland K area	Control
Ca (mg/mL)	24.3	2.7	14
Mg (mg/mL)	5.3	2.2	2.1
Cu (mg/mL)	< 0.01	0.03	0.003
Zn (mg/mL)	0.008	0.038	0.005
Fe (mg/mL)	0.04	0.05	< 0.03

* : $p < 0.05$

(population: 1,005,710 in the 2009 census) covers the southwest side of the Kii Peninsula. The Koza/Kozagawa/Kushimoto (K) area (population: 22,633 in the 2009 census, 430.3 km^2) is located in the southern part of the Kii peninsula. Oshima (population: 1,217 in the 2009 census, 9.93 km^2) is an island opposite the mainland K area and is municipally included in the K area. The water source of the mainland K area is the Kozagawa River. On Oshima, the source of drinking water had been regional rivers, wells and rainfall before 1975; however, this was changed to the Kozagawa River after waterworks were installed in 1975. Oshima is a rather isolated, hotel-free and restaurant-free rural area dependent in large part on locally produced food and fishing. There is a local public healthcare and welfare center, a local public hospital, two private hospitals and 19 medical clinics in the K area.

The control area is a small village, Hanazono, located in the northern part of the Kii Peninsula (Fig. 1). This is a mountainous area where people work in agriculture, forestry and recently tertiary industries. The water source is the local river, and there were no patients with ALS in this area between 1960 and 2009.

Measurement of mineral elements in the water

In 2009, two-liter water samples from waterworks (drinking water), a regional river and wells from the mainland K area, Oshima and the control area were collected in polyethylene bottles treated with 10% hydrochloride to prevent contamination. Drinking water samples were collected at four points in the mainland K area, three points on Oshima and three points in the control area. The concentrations of Ca, Mg, Mn and Fe were determined using inductively-coupled plasma spectrophotometry (ICP), those of Al, Cu, Zn, Mo, Se and Pb were determined using inductively coupled plasma-mass spectrometry (ICP-MS), and that of Hg was determined using atomic absorption spectrophotometry.

Measurement of elements in the serum and urine of residents and patients with ALS in the K area

Blood and urine samples were collected from healthy inhabitants over 60 years of age on Oshima and in the control area and patients with probable or definite ALS in the K area (K-ALS). The patients were diagnosed based on the El Escorial criteria for ALS (12) by neurologists in our team at Wakayama Medical University between 2000 and 2009. These participants underwent annual public regional medical examination checkups, including blood chemistry, and participated in this research voluntarily with informed consent. The urine and blood samples were obtained in the morning before breakfast (urine: between 06:30-07:30, blood: 09:00-10:30). The serum concentrations of Ca, inorganic phosphorus, intact parathyroid hormone (PTH), Zn, Cu and 8-hydroxy-2'-deoxyguanosine (8-OHdG) in the urine samples were determined. The methods used in this analysis were the orthocresolphthalein complexone (OCPC) method for Ca, the molybdic acid ultraviolet absorption method for inorganic phosphorus, electrochemiluminescence (ECLIA) for intact PTH, atomic absorption spectrophotometry for Zn and Cu and ELISA for 8-OHdG. The present research was approved by the ethics committee of Wakayama Medical University (No. 289) and the Kansai University of Health Sciences (No. 10-03).

Statistics

The differences in mean values and ratios were examined using a one-way analysis of variance, the unpaired t-test for continuous variables or the Mann-Whitney test. Two-sided p values of <0.05 were considered to be significant. The statistical analyses were conducted using the Statistical Package for the Social Sciences version 14.0 (SPSS Japan, Inc.).

Results

Measurement of mineral elements in the water

The mean concentrations of minerals in the drinking water on Oshima are shown in Table 1. The mean Ca level of the drinking water on Oshima was significantly lower than that observed in the control samples. The levels of Mg, Cu and Zn in the drinking water on Oshima were also low compared to those observed in the control samples. The concentrations of Fe, Al and Mn in the drinking water were not different between these areas (data not shown). The regional river and well water that was utilized for drinking on Oshima contained higher levels of Ca and Mg, similar to the control samples, than those observed in the Kozagawa River water and Kozagawa well water. The drinking water in the mainland K area also contained lower Ca levels than the control samples. Hg, Se, Pb and Mo were not detected in any water samples.

Table 2. Demography and Participants Examined

Area	Population > 60 y.o. (Male, Female) #	Participants (Male, Female)	%	Mean age (S.D.)
Control area	246 (89, 157)	51 (18, 33)	20.7	73.0 (7.6)
Oshima	632 (248, 384)	146 (32, 114)	23.1	74.5 (8.5)
Patients with ALS in the K area*	15 (8,7)	9 (6, 3)	60.0	65.3 (13.8)

#: the 2000 census, Japan

*: Patients with ALS in the Koza/Kozagawa/Kushimoto (K) area including Oshima between 2000-2009

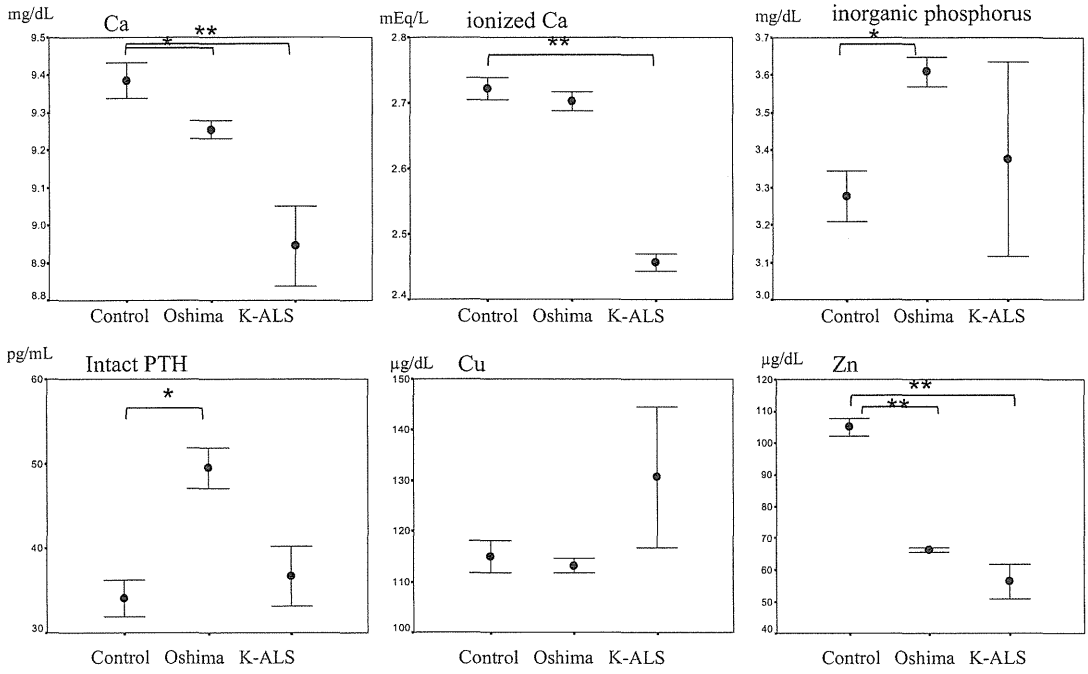

Figure 2. Serum concentrations of Ca (mg/dL), ionized Ca (mEq/L), inorganic phosphorus (mg/dL), intact PTH (pg/mL), Cu (μg/dL) and Zn (μg/dL) in the Oshima residents (O-residents), the ALS patients in the K area (K-ALS) and the controls.The serum Ca concentrations in the Oshima residents ($p<0.05$) and the patients with K-ALS ($p<0.01$) were lower than those observed in the controls. The mean serum concentrations of inorganic phosphorus and intact PTH in the Oshima residents were higher than those observed in the controls ($p<0.05$); meanwhile, the levels observed in the patients with ALS exhibited wide variation. The mean serum Zn concentrations in both the Oshima residents and patients with K-ALS were markedly lower than those observed in the controls ($p<0.01$, respectively). The bar indicates the mean±S.E.

Measurement of elements in the serum and urine of residents and patients with K-ALS

Fifty-one residents of the control area, 146 residents on Oshima and nine patients with K-ALS participated in this research (Table 2). Among the patients with K-ALS, the median duration between the onset of the first symptom and the measurement of elements was 36 months (range: 15 to 240 months). The patients with K-ALS exhibited lower Ca levels ($p<0.01$), lower ionized Ca levels ($p<0.01$) and lower Zn levels ($p<0.01$) than the controls. The intact PTH levels of the patients with K-ALS were not different from those of the controls, and the serum levels of inorganic phosphorus and Cu exhibited wide variation. In the residents of Oshima, the serum levels of Ca ($p<0.05$) and Zn ($p<0.01$) were also lower than those of the controls; however, the levels of inorganic phosphorus ($p<0.05$) and intact PTH ($p<0.05$) were higher than those of the controls, and the levels of ionized Ca were not different from those of the controls (Fig. 2). The Cu/Zn ratio, which is reported to be a marker of oxidative stress (13, 14), was higher in the patients with K-ALS and the Oshima residents than in the controls ($p<0.01$, respectively) (Fig. 3). The 8-OHdG level was determined in the patients with K-ALS (all nonsmokers) and non-smoking residents. The mean level of 8-OHdG in the patients with K-ALS was the highest among the three groups ($p<0.01$), and that of the Oshima residents was higher than that of the controls ($p<0.05$). The mean level of 8-OHdG/creatinine (adjusted for creatinine) was the highest in the patients with K-ALS among the three groups (Fig. 3).

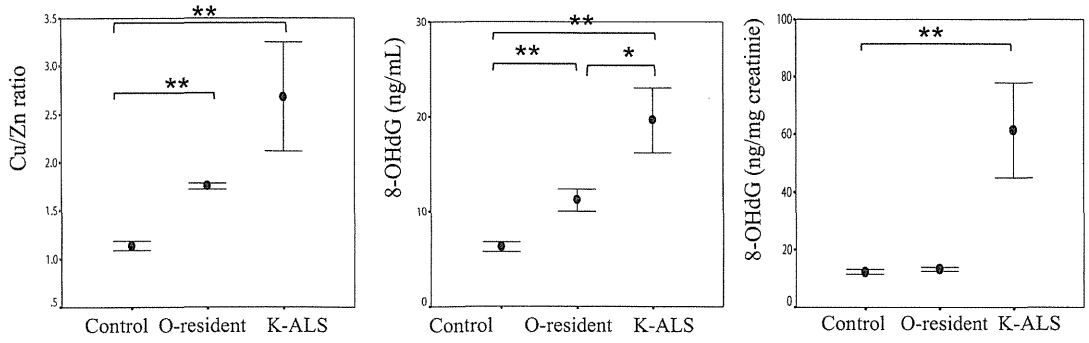

Figure 3. Cu/Zn ratios, levels of urinary 8-OHdG (ng/mL) and levels of 8-OHdG/creatinine in the patients with K-ALS and the Oshima residents (O-resident). The Cu/Zn ratios in the patients with K-ALS and the Oshima residents were higher than those observed in the controls ($p<0.01$, respectively). The mean concentration of 8-OHdG in the non-smoking Oshima residents (n=55) was higher than that observed in the non-smoking controls (n=35, $p<0.05$). The mean concentrations of 8-OHdG and 8-OHdG/creatinine in the patients with K-ALS (all nonsmokers, n=6, ng/mL) were the highest among the three groups ($p<0.01$). The bar indicates the mean±S.E. *: $p<0.05$, **: $p<0.01$

The contribution ratios of elements for variance among the patients with K-ALS, the Oshima residents and the controls were analyzed. The serum Zn levels and urinary 8 OHdG/creatinine levels exhibited high contribution ratios (0.60, 0.58, respectively) (Table 3). The serum Zn levels were significantly positively correlated with those of serum Ca (r: 0.72), inorganic P (r: 0.57) and Fe (r: 0.76) and negatively correlated with those of serum Cu (r: -0.61) in the patients with K-ALS. In the residents free from ALS, the serum Zn levels were positively correlated with the serum levels of Ca (r: 0.24), Fe (r: 0.31) and albumin (r: 0.42), similar to that observed in the patients with K-ALS, and negatively correlated with age (r: -179) and the levels of intact PTH (r: -0.24), inorganic P (r: -0.27) and urinary 8-OHdG (r: -0.25) (Table 4). The 8-OHdG/creatinine levels exhibited a positive correlation with the serum Cu levels in both the patients with K-ALS (r: 0.64) and the residents free from ALS (r: 0.32, $p<0.01$) and a negative correlation with the serum intact PTH levels (r: -0.74) in the patients with K-ALS.

Discussion

After the water supply was sourced from the Kozagawa River in the mainland K area in 1975, the drinking water on Oshima became markedly low in Ca, Mg, Cu and Zn, similar to that observed in the mainland K area (5, 10). Meanwhile, the water samples from wells and the regional river on Oshima, which had been used on Oshima before 1975, contained high levels of Ca and Mg.

The residents of Oshima exhibited lower serum Ca and Zn levels accompanied by higher inorganic phosphorus and intact PTH levels than the controls, while their ionized Ca levels were maintained at the levels observed in the controls. These results may be explained as a reaction to low intake of Ca and Zn. The low serum Ca and high intact PTH levels of the Oshima residents are compatible with our previous findings in residents of the Koza/Kozagawa area (a high-incidence area of ALS in which the drinking water contained markedly low levels of Ca) who exhibited low serum Ca levels regardless of sufficient intake from food, according to a self-administered food frequency questionnaire survey (15). Epidemiological studies of the relationship between tap water magnesium and calcium concentrations and various diseases have been conducted; however, conflicting results have been reported (16-18). Although prospective studies of metabolic balance, including the mineral levels in drinking water, food and serum, are necessary, the present findings in residents of Oshima may be partly explained by the recent change in drinking water source.

The patients with ALS in the K area exhibited severely low serum ionized Ca as well as serum total Ca and Zn levels without significant elevation of the intact PTH levels, which is significantly different from that observed in the Oshima residents. The low levels of intact PTH observed in the patients with K-ALS may be due to exhaustion of the parathyroid gland due to a possible longstanding Ca imbalance, wide fluctuation of the serum element levels or an unknown indigenous vulnerability in mineral metabolism, although the mechanisms were not clear.

The levels of Zn and 8-OHdG/creatinine explained 60% and 58% of the variance observed among the patients with K-ALS, the Oshima residents and the controls. Urinary 8-OHdG, an oxidized nucleoside of DNA, is excreted in the urine upon DNA repair and is regarded to be not only a biomarker of generalized cellular oxidative stress, but also a risk factor for cancer, atherosclerosis and diabetes (19). The levels of 8-OHdG/creatinine in morning spot urine are reported to correlate with the 8-OHdG levels in 24-hour pool urine (20). We herein reported for the first time that the morning spot urinary 8-OHdG and 8-OHdG/creatinine levels were significantly higher in the patients with ALS in the K